STM JOURNALS

Journal of
Polymer & Composites

ISSN: 2321-2810 (Online)
ISSN: 2321-8525 (Print)
Volume 12, Issue 6, 2024
DOI (Journal): 10.37591/JoPC

http://engineeringjournals.stmjournals.in/index.php/JoPC/index

Research JoPC

Synthesis, Characterization and Antibacterial Evaluation of Novel Canola Oil-Based Poly-(Citrate/Succinate)-amide Incorporated with Zn (II) and Ni (II) Metal Ions

Juhi Gupta[1], Md. Ikbal Ahmed Talukdar[2], Archana Chakravarty[3], Nitu Singh[4], Janesh Gautam[5], Suresh Sagadevan[6], Athar A. Hashmi[7,*]

Abstract

This present research study is to fabricate efficient metal-incorporated Canola oil (CO) polymers synthesised using dicarboxylic acids – Citric acid (CA) and Succinic acid (SA). The research mainly highlights the fabrication of polymeric materials using CO via a safer chemical synthesis route with less toxic reactants and minimal solvent/diluent to accomplish sustainability, adopting the green chemistry principle. Divalent Zinc (Zn) and Nickel (Ni) were incorporated in the poly-(Citrate/Succinate)-amide matrix, Ni being less explored till now. The composition, skeletal system and properties of Zn and Ni incorporated poly-(Citrate/Succinate)-amide were analysed by UV-visible, band gap energy, FTIR and NMR ($^{1}H/^{13}C$) spectroscopic studies along with their physio-chemical properties using standard methods. The size, stability and surface charge distribution were studied using DLS-Zeta, which has not been reported previously. Notably, the study established a slight comparison between the metal incorporated poly-(Citrate/Succinate)-amide. Metal-incorporated CO poly-(Citrate/Succinate)-amide were also examined for in-vitro antibacterial activity against Gram-positive (G+ve) B. cereus (MCC2243) and Gram-negative (G-ve) E. coli (MCC2412) bacteria using conventional procedures. The research analysis demonstrated that the antibacterial activity was enhanced when divalent Zn and Ni ions were introduced into the polymer matrix more than virgin canola oil, with more efficacy registered for Zn than Ni incorporated poly-(Citrate/Succinate)-amide and the mechanism for the same have also been discussed here. This research contributes to the development of sustainable biomaterials with promising applications as antibacterial coatings, biomedical and pharmaceutical, offering a greener and safer alternative to conventional synthesis methods.

***Author for Correspondence**
Athar A. Hashmi
E-mail: dr.aahashmi@yahoo.co.in

[1,2,4]Ph.D. Scholar, Bioinorganic Research Lab, Department of Chemistry, Jamia Millia Islamia, New Delhi, India
[3]Ph.D. Scholar, Department of Chemistry, Independent Researcher, New Delhi, India
[5]Scientist, ICMR, National Institute for Implementation Research on Non-Communicable Diseases, Jodhpur, Rajasthan, India
[6]Associate Professor, Nanotechnology and Catalysis Research Centre, University of Malaya, Kuala Lumpur, Malaysia
[7]Professor, Bioinorganic Research Lab, Department of Chemistry, Jamia Millia Islamia, New Delhi, India

Received Date: June 19, 2024
Accepted Date: July 30, 2024
Published Date: September 17, 2024

Citation: Juhi Gupta, Md. Ikbal Ahmed Talukdar, Archana Chakravarty, Nitu Singh, Janesh Gautam, Suresh Sagadevan, Athar A. Hashmi. Synthesis, Characterization and Antibacterial Evaluation of Novel Canola Oil-Based Poly-(Citrate/Succinate)-amide Incorporated with Zn(II) and Ni(II) Metal Ions. Journal of Polymer & Composites. 2024; 12(6): 45–69p.

Keywords: Canola oil, citric acid, succinic acid, metal incorporated polymers, zinc, nickel, biopolymers, biological activity, antibacterial activity

INTRODUCTION

Polymers have permeated every facet of modern life, sparking debate over their environmental impact on greenhouse gas emissions and toxic waste production. The eco-driven era's future global

economy, a circular bio-economy, safeguards raw resources and improves the environment by shifting from fossil fuels to renewables and sustainability is a priority [1–3]. After extensive debate over polymers' role in a sustainable, circular economy that prioritises environmental protection, resource conservation, and responsible waste management, novel methods for synthesizing complex macromolecular biodegradable polymers have evolved [2].

Vegetable oils are mostly used in food manufacturing sector. Non-edible vegetable oils usage have expanded substantially in the previous two decades, largely pushed by the polymer sector for centuries. Many different chemical reactions make use of vegetable oils; however, up until now, research into developing methods for producing chemical intermediates for biomaterial production from vegetable oils has mostly concentrated on soybean, castor, and linseed oils. Other main oilseed crops were comparatively underutilised in these attempts [4–8]. Various polymeric materials, including polyurethanes, thermosets, polyesters, polyamides, polyamines and their composites, have been developed from vegetable oils by adding polymerizable moieties such as acids, epoxy, amines or alcohol functionalities to the fatty acid structure with intriguing properties and prospective uses [2]. Depending on their specific properties, vegetable oils can be utilised in a broad range of products, including paints and coatings, biodiesel, adhesives, polymeric composites, cosmetics, plasticizers, bio-medical applications and many more [9]. As of present, CO have been converted into a wide variety of materials, including polymer nanocomposites, poly(ether ester) polyols, polyols, polyurethanes, interpenetrating polymer networks, methyl esters, thermoset epoxy resin, polyols, polyhydroxyalkanoates, water-reducible alkyds, etc. [8–14].

The chemical formula of CO is $C_{57}H_{106}O_6$ and the structure is described in Figure 1 [15]. CO is rich in monounsaturated fatty acids (MUFA) (58-63%), polyunsaturated fatty acids (PUFA) (30–35%), roughly twice of MUFA. The fatty acid content of CO includes 61% oleic acid (monounsaturated omega-9 fatty acid), 11% α-linolenic acid and 21% linoleic acid which are omega-3 and omega-6 PUFA and 7% saturated fatty acids. Its PUFA’s content is less than soybean, sunflower and maize oils but more than cottonseed, peanut and palm oils while oleic acid level is comparable to that of olive oil [16, 17]. Besides, it also contains phytosterols, tocopherols, which are biologically active isomers of vitamin E, beta-carotenes and chlorophylls. CO is "generally recognised as safe" (GRAS) and "heart-smart" for culinary utility by the US Food and Drug Administration (FDA), reducing possibility of coronary heart disease when substituted for saturated fats. By virtue of its biological activity and potential to reduce disease-related risk factors and promote health, CO has been hailed as a better option of edible vegetable oil [18]. Skin hydration and protection from external shocks are ensured by the skin's lipid barrier and CO's fatty acid profile implies that it might assist in maintaining this barrier [19]. CO, in comparison to sunflower oil, may help maintain a healthy lipid profile for cardiovascular health due to its greater omega-3 fatty acid concentration and lower saturated fat level. CO with low-erucic acid and high PUFA content cause less cardiopathologic changes while sunflower oil, with high MUFA (especially oleic acid) concentration, may be favoured for flavour and cooking [20, 21].

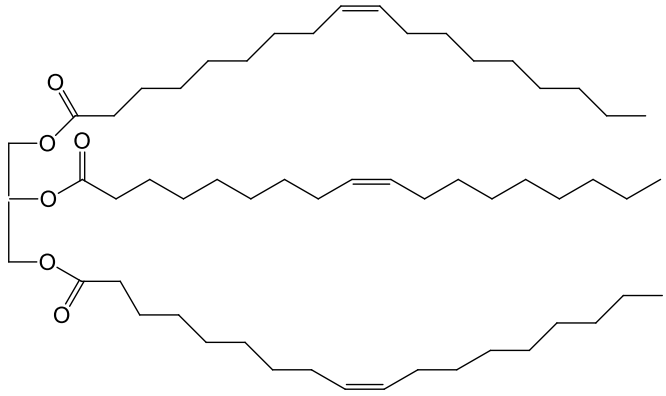

Figure 1. Chemical structure of canola oil [15].

High-performance organometallic polymers containing transition metals have attracted scientists owing to distinct physical and chemical properties, which opens up polymer science and engineering applications such as optics, biomedicine, aerospace, catalysis, thermal and electrical conductivity, adhesives, colourants, additives, resins, photonic and magnetic conductivity, etc. [22, 23]. Zn(II) is commonly employed in biomedical, antibacterial, antifungal and antiviral applications. Additionally, Ni(II) is used as an antibiotic, antifungal, antileukemia and biomedical implant [24].

Bacterial infections continue to be a leading cause of various diseases and mortality, despite the widespread availability of antibiotics and resistance towards antibacterial drugs is now common since many species have already evolved to this point [25]. Literature shows that incorporating metals in synthetic compounds and polymers boosts their antibacterial capabilities since wide range of structural alterations can be made to them owing their metal-ion releasing capacity at metabolically active areas of pathogens without relying on electron mobility to do so. Antibacterial properties are suggested by electron flow between metal-incorporated polymers and the bacterial surface and the degree of heterogeneity in structures in addition to the ability to disperse metal ions at pathogen hotspots [26, 27].

FDA-approved CA is a non-toxic, bio-based, readily accessible polycarboxylic acid with higher biocompatibility. CA forms covalent-ester intermolecular interactions with the polyol's hydroxyl group [28]. CA, an active proton donor, grows the polymer chain and facilitates branching at the ends as in the case of carboxymethyl chitosan and polyvinyl alcohol films, used for multipurpose food packaging were improved by CA cross linking in the amide diol matrix, which also promoted composite film breakdown by soil microorganisms [29, 30]. While, SA is an important part of many chemical processes, including the synthesis of polymers, resins, and solvents. SA, in addition to its usage as a nutritional supplement, is used as a food additive due to its acid-regulating characteristics. Because of its antioxidant properties, it is a sustainable alternative to improve the durability of biodegradable aliphatic polyesters [31]. SA's biotechnological manufacturing simplicity and capacity to synthesise a wide range of compounds contribute to its flexibility as a platform chemical. There is evidence that SA polyols have positive effects on human metabolism, and their incorporation into formulations provides a safe and cost-effective way to use renewable components [32].

Through the present article, we aim at helping societies become more sustainable. Our aim is simply to reduce waste and promote sustainable use of renewable resources, eco-design, toxic substances reduction and elimination and waste elimination. Their excellent stereochemistry, low toxicity, and high sustainability have spurred increased research into bio-origin compounds for antimicrobial action. All the reagents and materials used in the reaction are biodegradable and pose less toxicity to the environment. Herein, we have selected CO as our raw material and reported the formation of Zn and Ni incorporated CO-based poly-(Citrate/Succinate)-amide matrix via esterification reaction using two different dibasic acids. Ni has been least exploited for its utility as these poly-(Citrate/Succinate)-amide complexes. We carried out the base-catalyzed amidation reaction of CO with excess diethanolamine to yield CO-based fatty amide diol (hydroxyl functionality), followed by treatment with CA and SA (dibasic acids), which yielded CO-based poly(Citrate/Succinate)-amide resin. Utilizing the fluidity of the poly-(Citrate/Succinate)-amide resin, thereby acting as a diluent, was advantageous, thus minimizing solvent during the synthesis. The condensation reaction facilitates controlled and narrow molecular weight polymeric distribution during polymerisation.

The current study's objective was to describe and examine new metal coordinated poly-(Citrate/Succinate)-amide resin to be utilised as potential antibacterial agents. And, also, we have established a slight differentiation in the properties and activity between the resins obtained while using different acid precursors. The methodology proposes a potential alternative option for CO utilization to fabricate biobased antibacterial polymers that might have potential to be utilised in paints, packaging industries or as films with completely biodegradable antibacterial characteristics, etc. The primary biobased raw materials used are CO, CA/SA, however, there is scarce literature reports that provide

evidence on the fabrication of metal incorporated CO poly-(Citrate/Succinate)-amide system from these as raw materials and also characterize these polymers as antibacterial agents and, hence, these polymers have also been analysed for their applicability. The utilisation of Zn and Ni incorporated CO-based poly-(Citrate/Succinate)-amide as antibacterial agents has been little studied without known mechanism and incorporating natural acids will manage the durability and lifespan of the polymeric material. In the long run, these oil-based polymer complexes would eventually prove to be an efficient substitute of widely available petro-based polymers in the market.

MATERIALS AND METHOD

Refined Canola oil (RCO) was purchased from the local market. Diethanolamine (DA) (23105), P-toluenesulfonic acid (PTSA) (6101) were shopped from Fisher Scientific, New Delhi and Citric acid, Succinic acid, sodium metal, N, N-dimethyl formamide (DMF). Sodium chloride (41721) from SRL chem, diethyl ether (D0105) from Rankem. Zinc acetate and nickel acetate tetrahydrate from Loba chemie (608-89-9). All the reagents and chemicals were of analytical grade and simply utilised unaltered and without additional purifications.

Synthesis of Hydroxyethyl RCO Fatty Amide Diol / Monoglyceride (RCOM)

5 g of DA and approximately 3 ml of sodium ethoxide solution were taken in a three-neck round bottom (RB) flask equipped with thermometer, condenser and nitrogen inlet tube and was mixed thoroughly with the help of 5 MLH magnetic stirrer. The contents of the flask were heated up to 120°C. 6 g of RCO was added constantly with slowly rising temperature up to 150°C at 350-400 rpm stirring. RCO and DA were added in a 1:2 M ratio with only a little amount of DMF as solvent. The reaction was closely examined using TLC, acid value and FTIR spectroscopy. The moment when the acid value is positive and the required FTIR spectrum is obtained, the reaction was terminated. On subsequent cooling, obtained mixture was washed with 50 mL diethyl ether preceded by 15% brine solution and then kept overnight undisturbed. There were two layers that were segregated with the bottom layer being decanted off and the resultant less dense ethereal layer of the fatty amide was evaporated via rotary vacuum evaporator under reduced pressure and the final orangish yellow oily product was obtained followed by drying via anhydrous sodium sulphate.

Synthesis of Polyesteramide Resin (RCOPE)

With the same experimental set-up in a three-neck RB flask, 5 g of RCOM, 0.5 g CA/SA and up to 3 mL of DMF as solvent and 0.1 mg of PTSA (catalyst) were added and refluxed to 150°C. A similar method to RCOM was used to monitor until the target acid value was reached and the FTIR spectrum was obtained. After the completion of both the reactions, the mixture was cooled and similarly washed with diethyl ether and brine solution and then kept overnight till two layers separated in each separating funnel. The upper layer was purified with anhydrous sodium sulphate while the lower layer was discarded. The resultant purified products were then placed in rotary vacuum evaporator to remove any solvent content. The yellowish product so obtained was poly-(Citrate/Succinate)-amide resin and labelled RCOPE-(CA/SA) [RCOPE-(C/S)].

Synthesis of RCOPE-(C/S)-Zn and RCOPE-(C/S)-Ni

Dried RCOPE-(C/S) were taken in similarly equipped three-neck RB flask as above. 0.025 M Zn(II) i.e., 0.48g was added in fractions into the reaction mixtures RCOPE-(C/S) at 180–190 °C at 550 rpm for 5-6 h. Similarly, second loop of experiment was performed with 0.045 M Ni(II) i.e., 0.80g in small fractions in RCOPE-(C/S) at 180-190°C at 550 rpm and the evolution of all the reactions were monitored as RCOM. Two distinct layers marked the completion of the reactions alike RCOM. UV-Visible, FTIR and acid value measurements were taken at regular intervals till desired value is reached. Dark orange oily layer in flask A (RCOPE-(S)-Zn) and greenish black layer in flask B (RCOPE-(S)-Ni) with SA, while dark orangish compound in flask C (RCOPE-(C)-Zn) and dark greenish in flask D (RCOPE-(C)-Ni) with CA were obtained. Afterwards, they were extracted and refined using the same RCOM procedure described before (Figure.2).

CHARACTERISATIONS

Physico-chemical Characteristics

TLC and a determination of the physicochemical parameters are the primary methods that are utilised in order to track the development of the reactions throughout each and every step. Throughout the entire reaction scheme, acid value, hydroxyl value, iodine value and saponification value were measured using standard laboratory techniques. At room temperature, the soluble fractions of RCO, RCOPE-(C/S), RCOPE-(C/S)-Zn and RCOPE-(C/S)-Ni were trialled in a multitude of solvents.

Structural Analysis

To validate the formation of metal incorporated polymer complexes, UV-Visible spectroscopy is the easiest and most essential approach. The optical properties of the synthesised complexes were investigated using a Hitachi U3900 spectrophotometer covering the range 200-800 nm, with chloroform serving as a blank.

Surface functionalisation, vibrational bands, etc. present in the structure were determined by the FTIR spectra of the RCO, RCOPE-(C/S), RCOPE-(C/S)-Zn and RCOPE-(C/S)-Ni. The emission spectra were recorded at room temperature using a Bruker (Tensor 37, ranging 4000–400 cm^{-1}).

Solution-state nuclear magnetic resonance (NMR) spectral investigations were performed with deuterated chloroform (1 mL) as the solvent and tetramethylsilane (TMS) as the internal standard. Both ^{1}H and ^{13}C NMR spectra were collected at 30°C using a 500 MHz JEOL INDIA spectrophotometer (JNM ECX-500).

For the size distribution profile and behaviour and stability of the complex samples, Dynamic Light Scattering (DLS) and Zeta potential measurements were carried out using a Zetasizer Nano HPPSv420 (Malvern Instruments, Ltd., Malvern, UK) at 25 °C. Particle properties such as hydrodynamic diameter (z-average), polydispersity index (PDI), zeta potential values, electrophoretic mobility and width distribution were evaluated.

RESULTS AND DISCUSSION

Physico-chemical characteristics

The obtained values for physico-chemical characteristics are given in the following Table 1. From the data, it is clear that the data exhibit an increase in specific gravity and viscosity from RCO to RCOPE-(C/S)-Zn to RCOPE-(C/S)-Ni, while saponification and iodine value were inversely correlated. This reduction is mainly ascribed to increased fatty acid chain length thereby increasing molecular weight of the polymer and decreasing unsaturated content due to step-growth polymerization and metal coordination from RCOPE-(C/S) to RCOPE-(C/S)-M. The hydroxyl value first shows an increase from RCO to RCOM and then decrease from RCOM to RCOPE-(C/S) and then there is a slight increase from RCOPE-(C/S) to RCOPE-(C/S)-Zn/Ni. Slightly higher acid value in case of RCOPE-(C/S)-Ni than RCOPE-(C/S)-Zn and RCOPE-(C/S) indicate interaction of Zn and Ni acetates in the backbone of the RCOPE-(C/S), culminating higher molecular weight polymeric material with close packed array of metal coordinated poly-(Citrate/Succinate)-amide as compared to RCO as described in Figure 2, which are in strong agreement with the literature [33, 34].

Solubility test was carried out using different solvents on RCO, RCOPE-(C/S) and metal incorporated poly-(Citrate/Succinate)-amide [RCOPE-(C/S)-Zn/Ni] at room temperature (Table 2). In accordance with the results, RCOPE-(C/S) was immensely miscible with organic solvents like chloroform and acetone, as well as highly polar solvents like DMF, dimethylacetamide (DMA)and dimethyl sulfoxide (DMSO), but it exhibited poor miscibility in methanol, ethanol and formic acid whereas insoluble in water. RCOPE-(C/S)-Zn/Ni is soluble in the aforementioned solvents due to the covalent linkage between metal and oxygen thus rendering solubility in a vast range of solvents. The presence of mixture of polar groups and lengthy fatty acid hydrocarbon chains might be responsible for the solubility of the compound. Insolubility of these novel materials in water poses a significant challenge to the pharmaceutical and industrial product development methodologies.

Table 1. Physico-chemical characterization of RCO, RCOM, RCOP-(C/S), RCOPE-(C/S)-Zn and RCOPE-(C/S)-Ni.

Sample name	Acid Value	Saponification Value	Hydroxyl Value	Iodine Value
RCO	0.0723	192.3	–	114.6
RCOM	2.751	167.2	254.8	55.3
RCOPE-(C)	3.072	136.5	101.9	22.1
RCOPE-(S)	3.037	135.8	102.1	24.3
RCOPE-(C)-Zn	3.8241	128.2	68.1	18.5
RCOPE-(S)-Zn	3.762	128.3	65.5	16.2
RCOPE-(C)-Ni	4.579	126.4	67.9	17.7
RCOPE-(S)-Ni	4.2639	127.9	67.7	17.4

Table 2. Solubility results of RCO, RCOPE-(C/S) and RCOPE -(C/S)-Zn/Ni with some common solvents (where I: Insoluble, PS: Partially Soluble and S: Soluble).

Sample name	Solvents								
	Water	***Acetone***	***Chloroform***	***Methanol***	***Ethanol***	***DMF***	***DMA***	***DMSO***	***Formic acid***
RCO	I	S	S	I	I	I	S	S	I
RCOPE-(C/S)	I	S	S	PS	S	S	S	S	PS
RCOPE-(C/S)-Zn/Ni	I	S	S	S	S	S	S	S	PS

SPECTRAL ANALYSIS

FTIR Spectroscopy

The FT-IR spectra of metal-incorporated poly-(Citrate/Succinate)-amide systems are shown. The primary peaks for RCO are as follows: 1732 cm^{-1} for the C = O triglycerides' ester group, 1621 cm^{-1} for C = C, 2928 cm^{-1} and 2855 cm^{-1} for the asymmetric and symmetric vibrations, respectively and 1465 cm^{-1} for the bending vibrations of the -CH bond. $-CH_2$ rock is responsible for the strong peak that can be found at around 722 cm^{-1}. The coordination of RCOPE with Zn and Ni is indicated by the fingerprint peaks in the range of 480-590 cm^{-1} for RCOPE-(C/S)-Zn and RCOPE-(C/S)-Ni. The incorporation of Zn and Ni in CO framework is strongly indicated by the reduction in the strength of the hydroxyl peak and the shift in the C = O ester and C = C triglyceride chain peaks. The hydroxyl group in RCO is represented by the band at 3400 cm^{-1} [35], whereas the appearance of this same value in the spectra of RCOPE-(C/S)-Zn and RCOPE-(C/S)-Ni with lower intensity shows the interaction of the hydroxyl group (OH) with the dimeric acid and, in turn, with Zn and Ni. In RCO, the ester (saturated) linkage is responsible for the peak at 1735 cm^{-1}, while the peak at 1657 cm^{-1} is related to the CH=CH stretching vibration of the double bond (Figure 3).

UV-Visible Spectral Analysis

UV spectrum of RCO, RCOPE-(C/S)-Zn and RCOPE-(C/S)-Ni is described in Figure 3. The peaks at 233 and 330 nm is due to n→л* and л→л* transitions respectively in the crude oil. The sharp, intense intra-ligand charge transfer peaks show analogy with the crude oil with peaks at 259 and 347 nm; 242 and 335 nm; 269 and 340 nm for the RCOPE-(C)-Zn, RCOPE-(S)-Zn and RCOPE-(S)-Ni respectively. However, peak broadness in case of RCOPE-(C)-Ni might have led to the mergence of both the peaks.

While Figure 2 also shows interaction of canola oil with divalent metal ions like Zn(II) and Ni(II) with different polymerising acid. Coordination between transition metal and polymer matrix should cause UV-Visible spectra of complexes to show absorption band position that differentiates from those of crude oil and related complexes. Since, RCO does not appreciably absorb above 330 nm hence, new absorption maxima are seen as evidence of complex formation [36]. The broader and medium absorption peaks at 400 and 415 nm may arise from the charge-transfer transition from the ligand to

metal ions (LMCT) due to Ni ions in RCOPE-(C/S)-Ni. Increased intensity in case of RCOPE-(S)-Ni might be the result of combination of л→л* and charge transfer peak. Absorption around 400–600 nm in the metal complex spectrum can be attributed to either the d-d transitional bands of the metal or charge transfer from the ligand to the metal. For RCOPE-(S)-Ni, intense shoulder at 415 nm with a small component/ broader peak at 432 nm ($^2A_{1g}\rightarrow{}^1B_{1g}$) which tails down to cut-off at 470 nm ($^1A_{1g}\rightarrow{}^1A_{2g}$) is observed which indicate d-d transitions [37]. Weak intensity of the LMCT transitions may arise due to the complexity of the polymeric structure. While in Zn complexes, no d-d transition was observed. The complexes of Zn(II) displayed high intensity hyperchromic bands at around (250-280 nm) and (320-350 nm) that are expected for d^{10} and d^0 configurations. A large number of metal organic frameworks with zinc ions generally have filled d sub-shell thereby rendering no d-d transitions [38]. From the spectra, it might be estimated that metal incorporation has elevated the intensity of the transition metal complexes than the crude oil.

In this regard, we propose a square planar geometry for the RCOPE-(C/S)-Zn complex and distorted square planar geometry for the RCOPE-(C/S)-Ni [39, 40]. The formation of the poly-(Citrate/Succinate)-amide complexes is well supported by the UV spectrum and it became evident on comparing it with RCO.

Band gap energy of a semiconductor describes the amount of energy required to excite an electron from the valence band to the conduction band. Predicting the photophysical and photochemical characteristics of semiconductors requires an exact estimate of the band gap energy. The equation, $(\alpha h\upsilon)^m = k(h\upsilon - E_g)$, often known as the Tauc and Davis-Mott relation, is used to determine the optical band gap energy of all complexes using UV-Visible spectroscopy. All the band gap calculations have been found using direct allowed transitions (Figure 5). The estimated energy gap thus obtained for RCOPE-(C)-Zn and RCOPE-(S)-Zn equals 4.04 eV and 4.24 eV respectively, while that for RCOPE-(C)-Ni and RCOPE-(S)-Ni is 3.48 eV and 3.35 eV respectively.

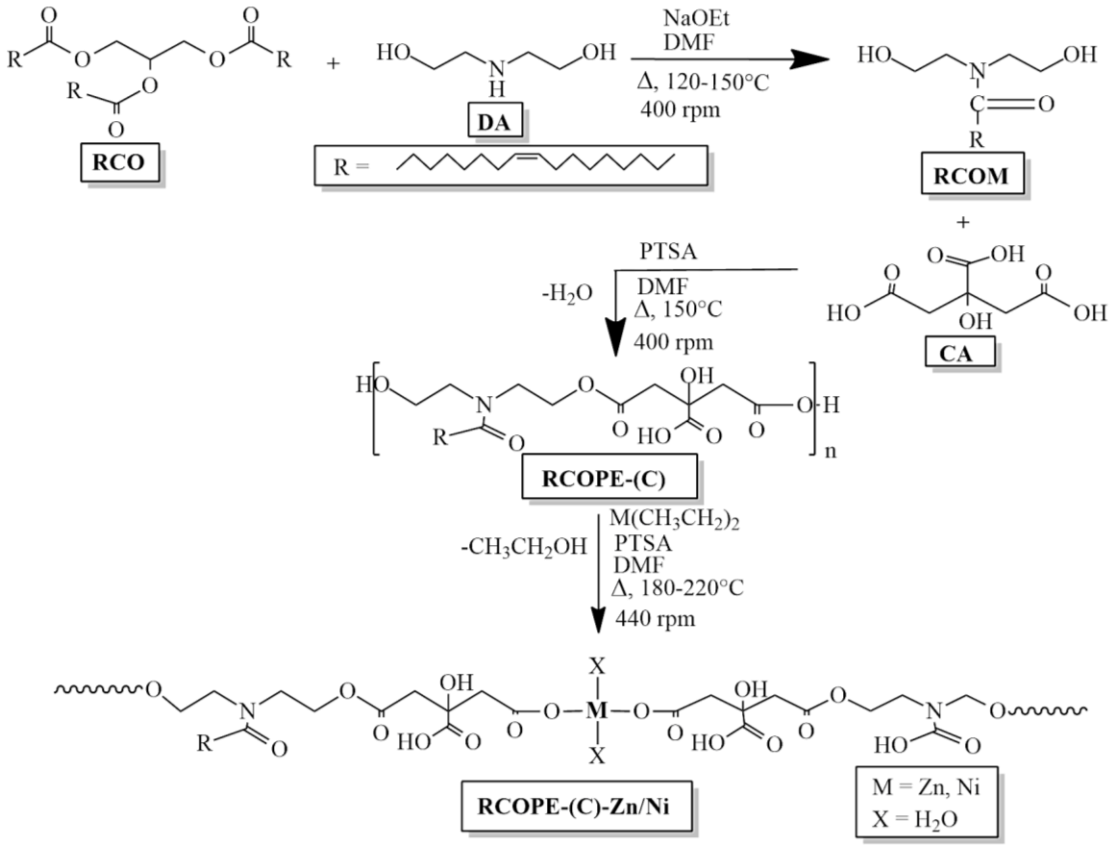

Figure 2. Schematic representation of synthesis of canola oil based metallic poly-(Citrate/Succinate)-amide using citric acid (similarly for succinic acid).

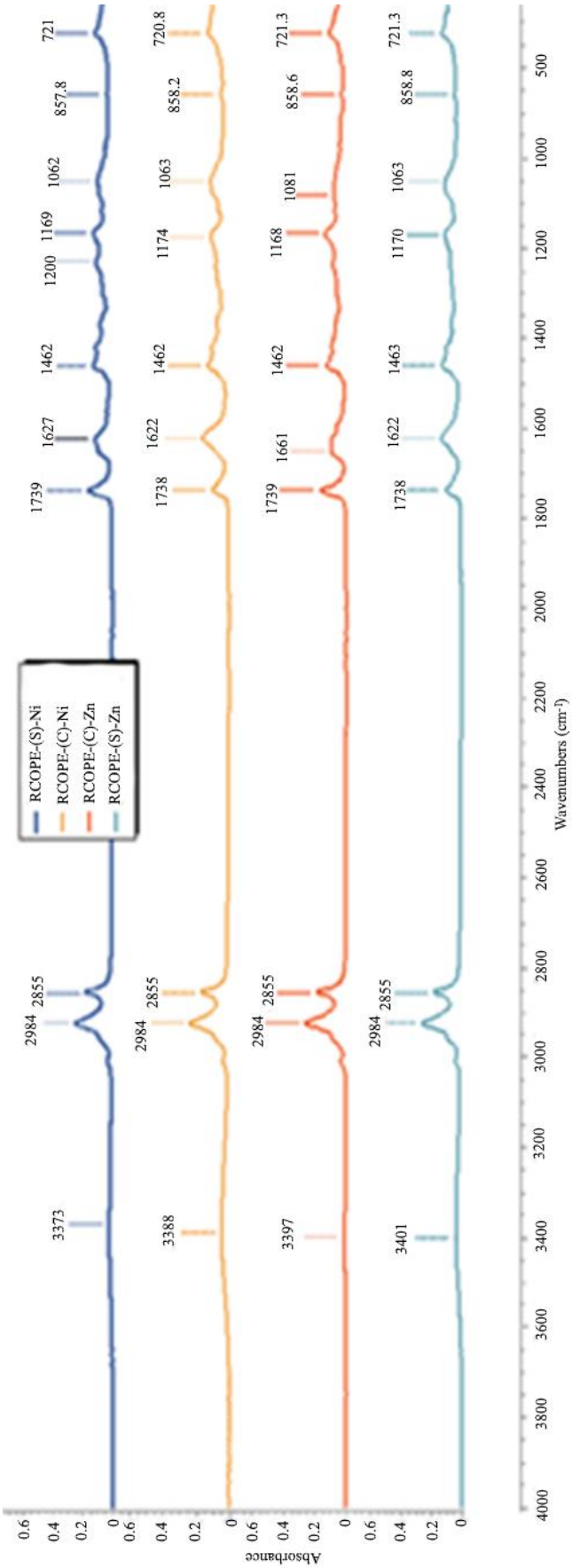

Figure 3. FTIR spectrum of RCOPE-(C)-Zn, RCOPE-(C)-Ni, RCOPE-(S)-Zn and RCOPE-(S)-Ni.

Apparently, inspection of results revealed that the synthesised complexes had a lower energy gap than RCO (E_g = 4.28 eV). The d-orbitals of Ni^{2+} and the LUMO of the polymeric matrix combine to create lower conduction bands, resulting in a smaller energy gap compared to that of Zn^{2+}. Theoretically, upon complexation, the metal's ability to accept electrons into its shell increases their mobilization. After complexation, it is possible to observe that the chemical structure of RCO changes, the localized level widths widen and the band gap shrinks. Due to the reduced optical band gap in case of synthesised PEA complexes might have possibility to have substantial implications for electrical and optoelectronic device applications [41].

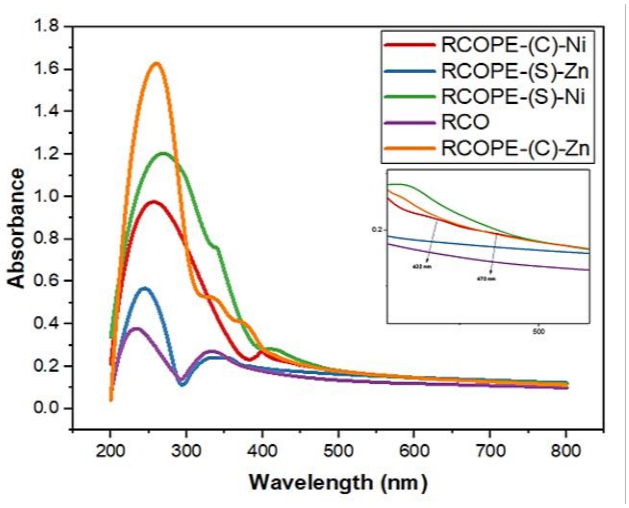

Figure 4. UV-Visible spectra of RCOPE-(C)-Zn, RCOPE-(C)-Ni, RCOPE-(S)-Zn and RCOPE-(S)-Ni.

Table 3. Different chemical shift values of ^{1}H NMR peaks of RCO, RCOPE-(C/S)-Zn/Ni.

S. No.	Type of proton	RCO	RCOPE-(C)-Zn	RCOPE-(C)-Ni	RCOPE-(S)-Zn	RCOPE-(S)-Ni
1.	Terminal -CH_3	0.86	0.88	0.86	0.86	0.89
2.	Aliphatic -CH_2	1.26	1.29	1.25	1.27	1.31
3.	-CH_2-C=C-	1.99	2.03	1.98	2.00	2.04
4.	>N-CO-CH_2		2.32	2.30	2.36	2.31
5.	-CH_2-COO-	2.28	2.79	2.75	2.75	2.78
6.	-CH_2-N<		3.66	3.63	3.63	4.14
7.	-OCH_2 / -NCH_2CH_2O-	3.88	4.13-4.23	4.09-4.23	4.18	4.29-4.33
8.	-CH=CH-	5.32	5.35	5.31	5.32	5.34
9.	-OH		4.75	4.57	4.70	4.60

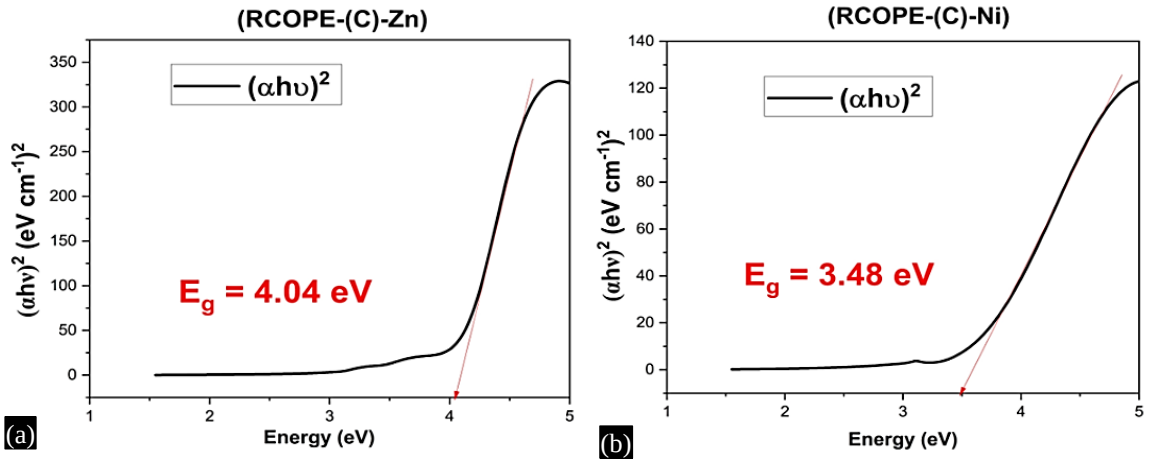

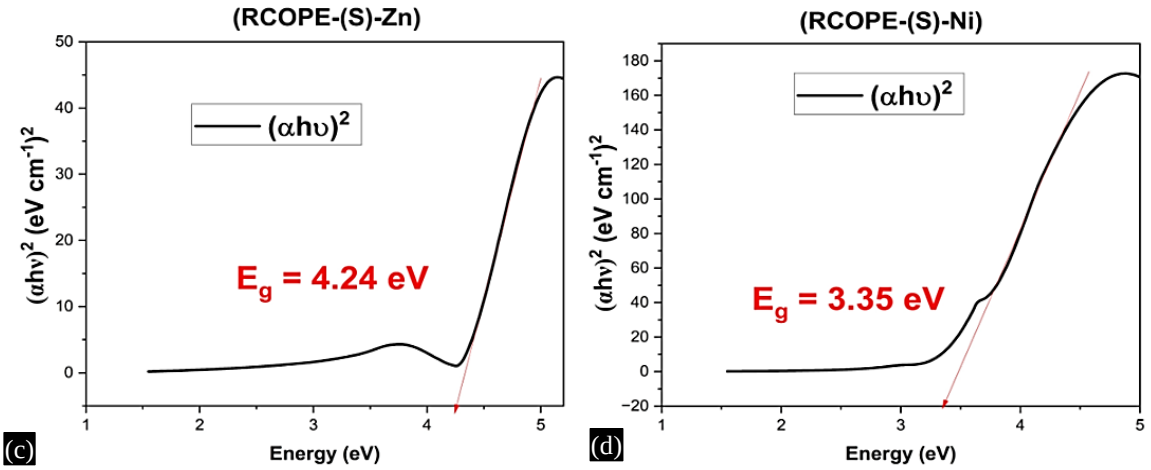

Figure 5. (a–d) Plots of $(\alpha h\nu)^2$ vs. Energy of RCOPE-(C)-Zn, RCOPE-(C)-Ni, RCOPE-(S)-Zn and RCOPE-(S)-Ni.

^{1}H and ^{13}C NMR Spectroscopy

NMR spectral comparisons provided additional evidence of the structure of the polymeric resins. ^{1}H NMR spectrum of the compounds have been mentioned below:

The chemical shift (δ) values of the protons of RCOPE-(C/S)-Zn/Ni at different assigned peaks are shown in Table 3 and the obtained δ are different and more complex than RCO. ^{1}H NMR spectral graph of RCOPE-(C)-Zn, RCOPE-(C)-Ni, RCOPE-(S)-Zn and RCOPE-(S)-Ni were shown in Figures 6 and 6. ^{13}C NMR of all the complexes and the refined oil was obtained as follows given in Table 4(Fig.7) below:

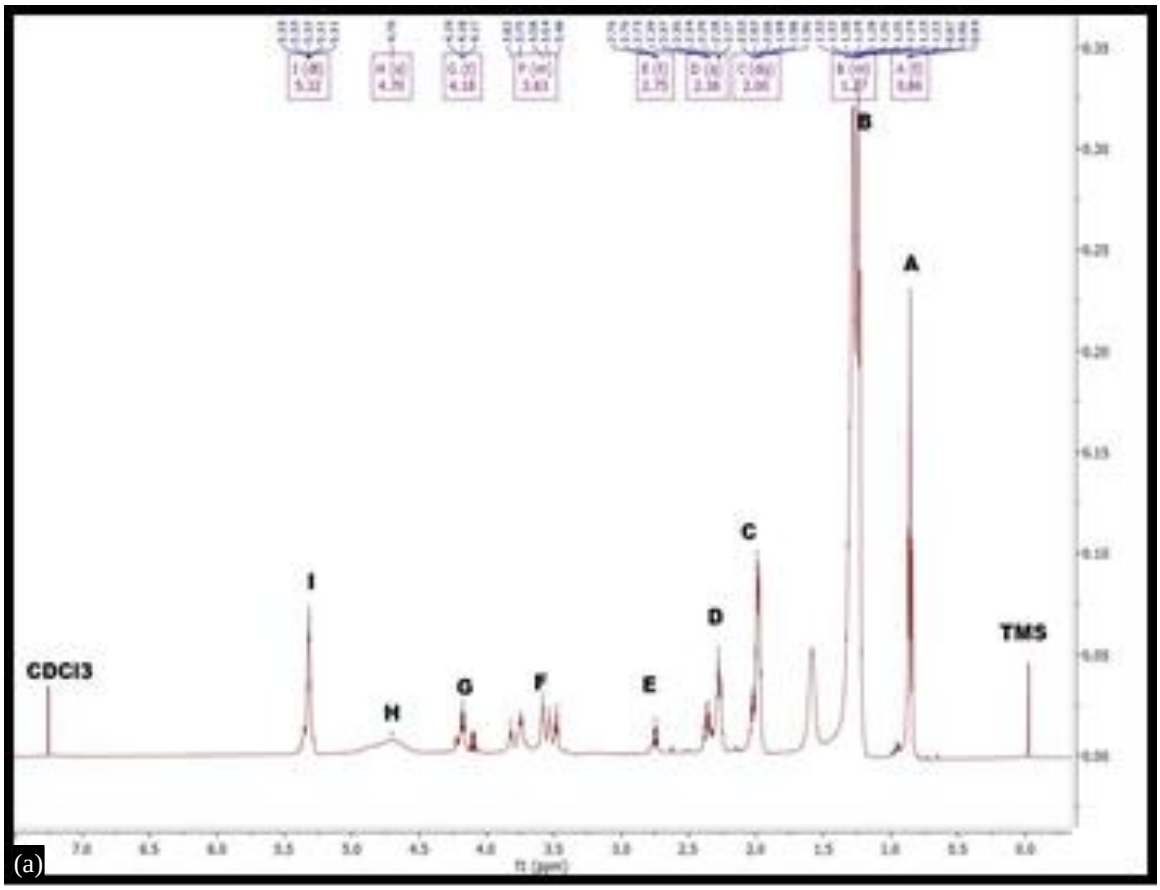

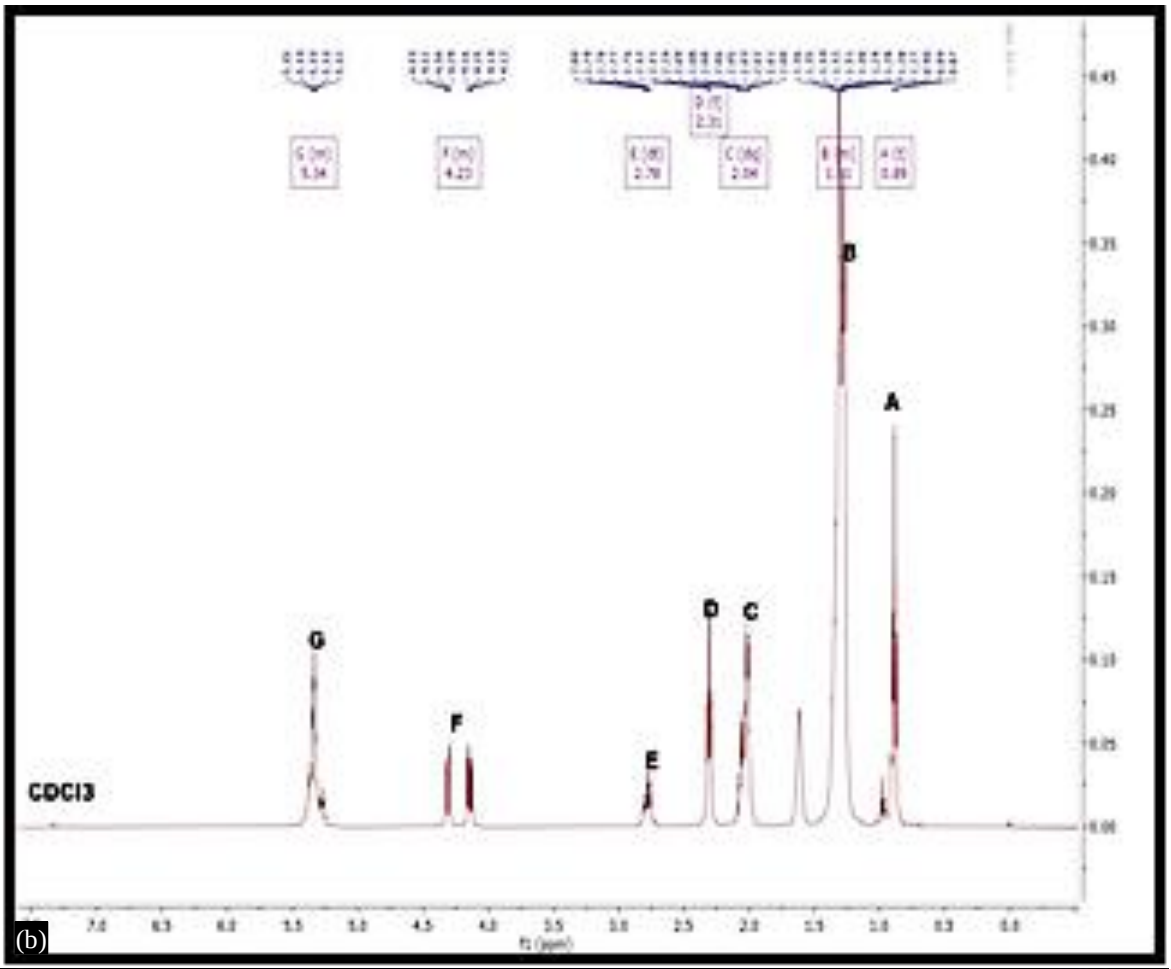

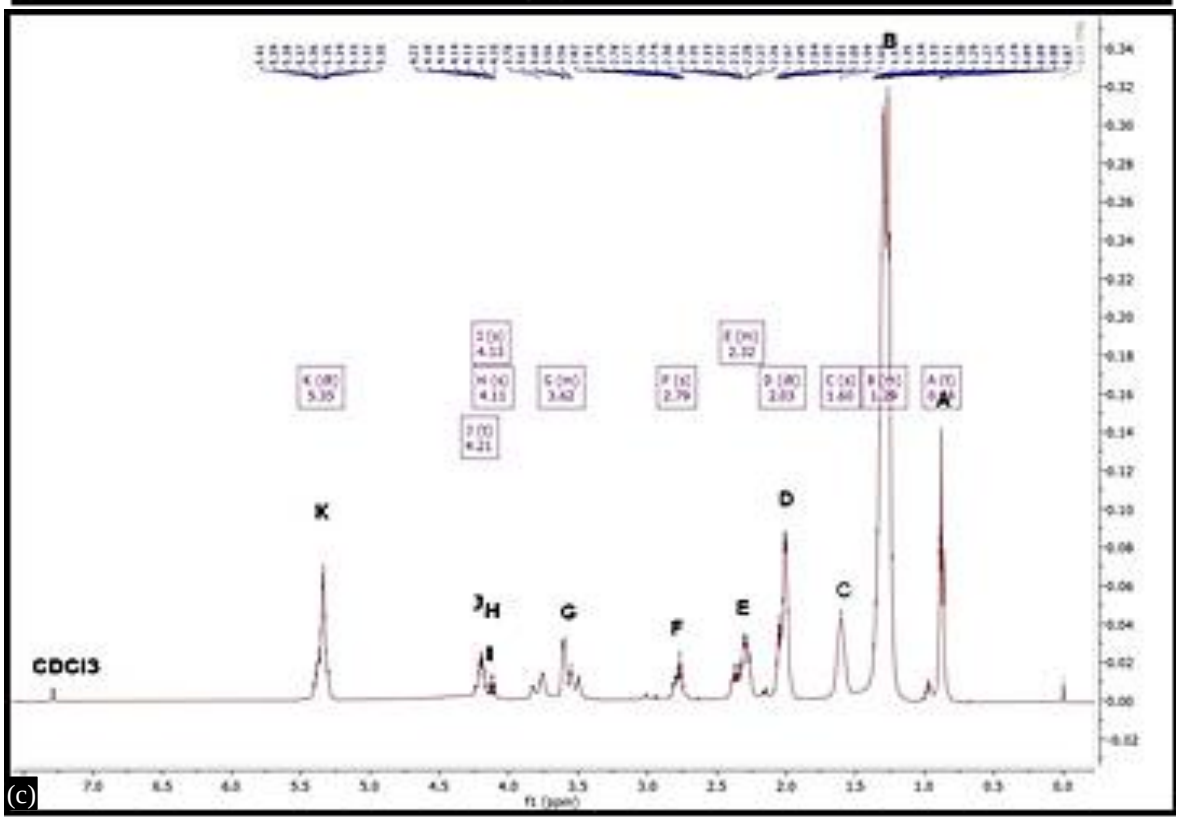

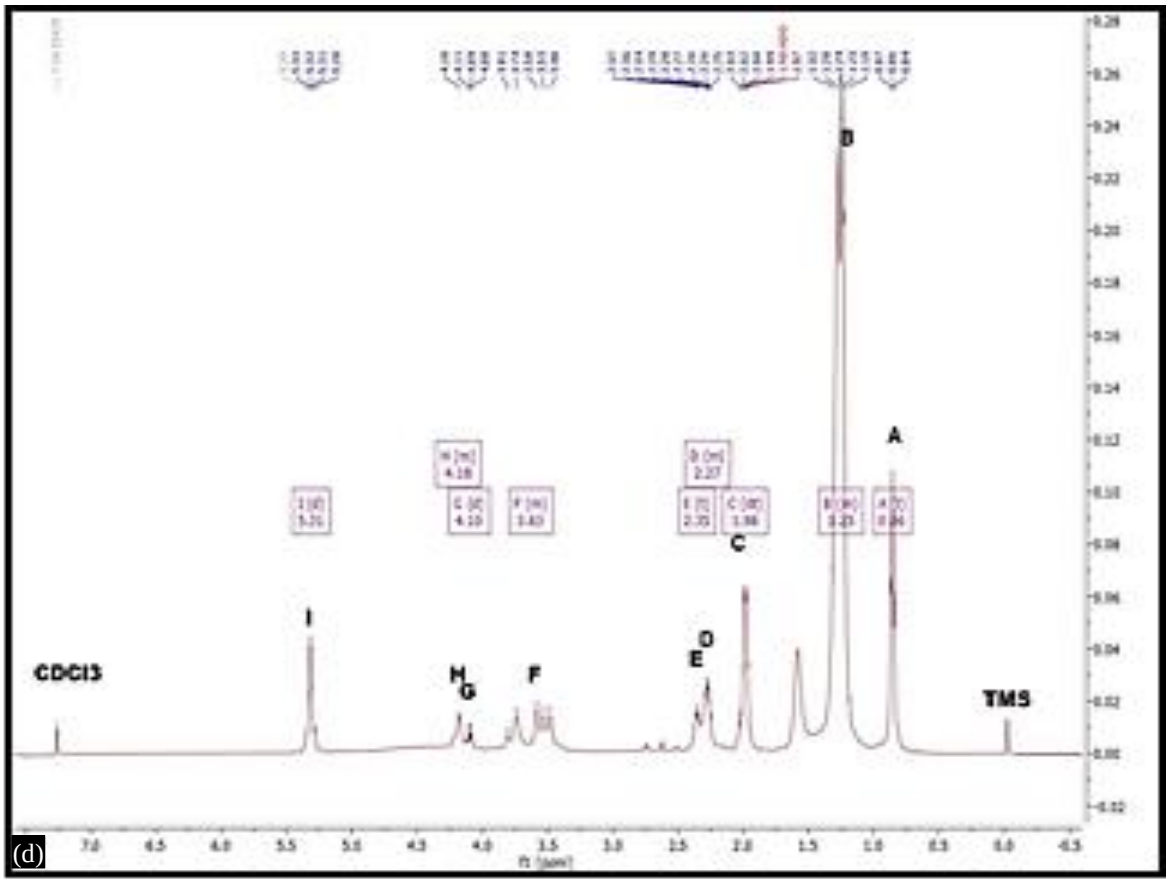

Figure 6. ^{1}H NMR spectral graph of (a) RCOPE-(C)-Zn, (b) RCOPE-(C)-Ni, (c) RCOPE-(S)-Zn and (d) RCOPE-(S)-Ni.

Table 4. Different chemical shift values of ^{13}C NMR peaks of RCO, RCOPE-(C/S)-Zn/Ni.

S. No.	Type of carbon	RCO	RCOPE-(C)-Zn	RCOPE-(C)-Ni	RCOPE-(S)-Zn	RCOPE-(S)-Ni
1.	Terminal -CH_3	13.84-14.3	14.31-14.36	14.13	14.20-14.24	14.19
2.	Aliphatic -CH_2	22.57-25.63	24.87-25.68	22.81-25.67	22.68-25.72	22.74
3.	-OCH_2CH_2-	27.19-27.2	27.28-27.30	27.20-27.30	27.28-27.32	27.26
3.	-CH_2-C=C-	29.05-29.84	29.06-29.85	29.12-29.83	29.25-29.87	29.18
4.	>N-CO-CH_2	- -	33.22-35.72	31.57-34.15	31.62-34.54	31.95-37.45
6.	-CH_2-N-CO-	- -	45.38-47.77	52.01-56.09	43.11-45.99	47.26
7.	-OCH_2	62.06-68.9	60.25-62.05	62.06-68.94	61.64	62.08
8.	-CH=CH-	127.13-131.81	127.94-130.27	127.14-132.38	129.86-130.10	129.77-139.63
9.	>C=O (amide)	- -	173.56-173.7	172.62	167.93-171.17	173.72
10.	>C=O (ester)	172.62-173.03	175.62	173	174.41	185.69

Clearly, the data is so obtained is different from RCO, suggests that the suggested technique, which involves metal introduction into the main poly-(Citrate/Succinate)-amide chain, is feasible. Nevertheless, both the data obtained are in accordance with the UV-Visible and FTIR spectral analysis.

Particle Size and Zeta Potential Measurements

Using DLS, we were able to quantify the particle size of the synthesised samples. DLS – Zeta potential studies (Table 5) showed the average mean diameter of RCOPE-(C)-Zn, RCOPE-(C)-Ni, RCOPE-(S)-Zn and RCOPE-(S)-Ni to be 1764, 577.6, 1402 and 395.6 nm respectively in the range of 350-2000 nm with zeta (ζ)- potential of -7.05, -3.76, -17 and -1.4 respectively. The apparent capping of

the bio-organic components present might explain the negative potential value reported. The regulation of particle aggregation or flocculation within the fluid is greatly influenced by ζ-potential. The negative ζ-potential may help toward its stability via minimizing its aggregation due to electrostatic repulsion [42]. ζ-potential is more negative for Zn-polymer complexes than Ni-polymer complex. Rise in the absolute value of the ζ-potential is indicative of decreased stability, which may lead to agglomeration of the particle, which may be connected with the growth in particle size of complexes while certainly a little incipient instability might have occurred in RCOPE-(S)-Zn. The average hydrodynamic particle diameter of RCOPE-(C)-Zn, RCOPE-(C)-Ni, RCOPE-(S)-Zn and RCOPE-(S)-Ni in methanol shows particle aggregation. Particle size and ζ-potential are fundamental for colloidal system stabilization. As from the data, all systems showed negative superficial electrical density suggesting that the surface is negatively charged and dispersed in the medium since fatty acids chain's extreme end is composed of carboxylic acid groups [43–45]. However, increased amplitude of interparticle interactions, suspensions with values less than 25 mV and the obtained hydrodynamic diameter of RCOPE-(C)-Zn, RCOPE-(C)-Ni, RCOPE-(S)-Zn and RCOPE-(S)-Ni in methanol exhibit a significant degree of agglomeration and flocculation. Thus, it might be concluded that more negative charge is imparted by RCOPE-(C/S)-Zn than RCOPE-(C/S)-Ni**.** Better ionic conductivity might be concluded for RCOPE-(C)-Zn and RCOPE-(C)-Ni than RCOPE-(S)-Zn and RCOPE-(S)-Ni [46, 47].

PDI Index may be used to characterise the distribution of particle sizes. The value of the PDI can vary from 0 to 1.0, with 0 to 0.3 representing the state of distribution with the maximum degree of homogeneity (mono-dispersed particles) [47, 48]. From the data, we can conclude RCOPE-(S)-Ni has the highest homogeneity followed by RCOPE-(C)-Ni and RCOPE-(S)-Zn and diverse particle size distribution of the formulation is of RCOPE-(C)-Zn.

Table 5. Zeta potential and Zeta size distribution data of RCOPE-(C)-Zn, RCOPE-(C)-Ni, RCOPE-(S)-Zn and RCOPE-(S)-Ni in methanol at room temperature.

Sample Name	Zeta potential distribution			Size distribution data	
	ZP[1] ± SD*	***Mob[2] ± SD****	***Cond[3] ± SD****	***Z-Avg[4] ± SD****	***PDI[4] ± SD****
	mV	*μm.cm/Vs*	*mS/cm*	*d.nm*	
RCOPE-(C)-Zn	-7.05 ± 0.59	-0.3762 ± 0.032	0.1097 ± 0.0004	1764 ± 273.2	0.86 ± 0.169
RCOPE-(C)-Ni	-3.76 ± 0.45	-0.2008 ± 0.024	0.213 ± 0.0021	577.6 ± 26.56	0.432 ± 0.035
RCOPE-(S)-Zn	-17 ± 0.37	-0.9053 ± 0.020	0.123 ± 0.0008	1402 ± 106.7	0.456 ± 0.046
RCOPE-(S)-Ni	-1.4 ± 0.54	-0.0747 ± 0.029	0.096 ± 0.0036	395.6 ± 63.18	0.228 ± 0.013

*Where, * SD: Standard Deviation; 1: Zeta Potential; 2: Mobility; 3: Conductance; 4: Z-Average; 5: Poly Dispersity Index.*

ANTIBACTERIAL ACTIVITY

Bacterial Strains and Growth Conditions

Antimicrobial activity against G+ve and G-ve bacteria was evaluated in all experiments [49]. The agar-well diffusion technique examined the bacteria's susceptibility to compounds. The G+ve bacteria *B. cereus* (MCC2243) and the G-ve bacteria *E. coli* (MCC2412) was inoculated by cultivating a raising the turbidity of a nutrient broth culture from a single colony to 0.5 McFarland units. Using a stock solution of 1000 g mL^{-1}, different doses of synthetic compounds (10, 20, 30, 40 g mL^{-1}) were plated on 25 mL Mueller Hinton agar medium plates containing bacterial cultures. The antibacterial activity of the samples was tested while they were still in solution and standard antibiotic (10 μg mL^{-1}) was used as a comparison. For 24 hours, these plates were incubated at 37°C. The data was reported as the mean (SD) inhibition zone diameter in millimetres. Each experiment was done three times. Antimicrobial efficacy was evaluated by measuring the size of the halo formed around the wells.

Zone of Inhibition

The Zone of Inhibition Test is a fundamental microbiological trial study majorly utilized in the medical device and pharmaceutical sectors. Screening antimicrobial products for inhibitory action against several bacteria is possible with its quick analysis.

Most tested materials allow the antibacterial to drain out, which is ideal. Simple and affordable, the Zone of Inhibition Test (also known as the Kirby-Bauer Test, Antimicrobial Susceptibility Test, Disk Diffusion Test, or Agar Diffusion Test) measures the antimicrobial activity of a substance or solution against the target bacteria. In 1961, the World Health Organization defined a test called the zone of inhibition. With increase in the concentration of samples the antibacterial resistances increase as shown in Figure 8, both Zinc & Nickel incorporated PEA; RCOPE-(C)-Zn & RCOPE-(C)-Ni, Zinc & Nickel incorporated poly-(Citrate/Succinate)-amide via citric acid modifications into polymerization have shown enhanced bactericidal effects with increasing in concentration. Virgin oil as such has not shown the same be its lower, mid, or even at high concentration. On comparison of RCOPE-(C)-Zn & RCOPE-(C)-Ni, RCOPE-(C)-Zn has shown better bacterial resistance with increasing in concentration then the RCOPE-(C)-Ni. These results can be attributed due to the better ion forming tendences of Zinc in complex forms than Nickel. The ion forming tendences of metal in complex forms are quite well known for both but the reactive oxygen species (ROS) along with metal ions forming tendencies have played the vital role for the bactericidal effects in Zinc & Nickel fabricated polymer samples and RCOPE–(C)-Zn has shown better at it than RCOPE-(C)-Ni. The linear, exponential and moving average trendline at a period of two are following the same for both the samples.

Similar to RCOPE-(C)-Zn & RCOPE-(C)-Ni, the zinc & nickel coordinated polymers, RCOPE-(S)-Zn & RCOPE-(S)-Ni, modified with succinic acid during polymerization, have improved bactericidal activity with increased concentrations. It is important to remember that virgin oil as a whole has not shown the same benefits regardless of its high, medium, or low concentration. A comparison of RCOPE-(S)-Zn & RCOPE-(S)-Ni indicates that RCOPE-(S)-Zn is better at preventing bacterial growth than RCOPE-(S)-Ni. A better ion forming tendency of Zinc in complex forms can explain these results. For both metals, ion formation tendencies are well known, but it is the ROS as well as metal ion forming tendencies that play the crucial role in the bactericidal effects of zinc & nickel polymer samples and RCOPE-(S)-Zn is more effective than RCOPE-(S)-Ni. The linear, exponential and moving average trendline at a period of two are following the same for both the samples as showed in Figure 9. Furthermore, these results are consistent with those of our prior work [26].

Antibacterial Results, Discussion and Mechanism

The efficacy of synthetic RCOPE-(C/S)-Zn and RCOPE-(C/S)-Ni as antibacterial agents in aqueous solution against G+ve (*B. cereus*, MCC2243) and G-ve (*E. coli*, MCC2412) bacteria was assessed. For each bacterial strain tested, no inhibitory zone was detected when tested against the virgin canola oil component (RCO), indicating that RCO alone lacks antibacterial action. Additionally, the bactericidal nature of the antimicrobial activity for RCOPE-(C/S)-Zn and RCOPE-(C/S)-Ni has been shown. All of them were very susceptible to both G+ve and G-ve bacteria (*B. cereus* and *E. coli*). When the concentration of RCOPE-(C/S)-Ni material was raised from 10 to 40 $\mu g\ mL^{-1}$, antibacterial activity was found to rise and it was shown to be most effective against *E. coli* and least effective against *B. cereus*. While comparable findings were shown for RCOPE-(C/S)-Zn. At higher concentrations of RCOPE-(C/S)-Zn material (10-40 μgmL^{-1}), RCOPE-(C/S)-Zn has demonstrated superior effectiveness against G+ve and G-ve bacteria when compared to RCOPE-(C/S)-Ni.

Figure 10 shows the proposed antibacterial mechanism for the efficient bactericidal effects by depleting probable ROS such as Zn^{2+}, Ni^{2+}, O^{2-}, OH^{-}, O_2^{2-}. These factors are responsible for the growth and antibacterial resistance of RCOPE-(C/S)-Zn & RCOPE-(C/S)-Ni polymer complexes. As shown in figure 10, metal ions' increased interaction with infectious microbes may explain why all the complexes were shown to have antibacterial activity against *B. cereus* and *E. coli*. The reason why RCOPE-(C/S)-Ni and RCOPE-(C/S)-Zn are more effective at killing bacteria is because (i) the polymer coating makes the metal ions stable and stops them from escaping (ii) electrostatic interaction between the metal ion

and the microorganism, leading to the stimulation of electron transport and oxidative phosphorylation at the cell membrane (iii) furthermore, this electron transport led to the generation of ROS, antimicrobial agents such OH^- and O^{2-}, which interacted with the bacterial cell wall that aid in the rupturing of the cell and induce antibacterial activity [26, 27].

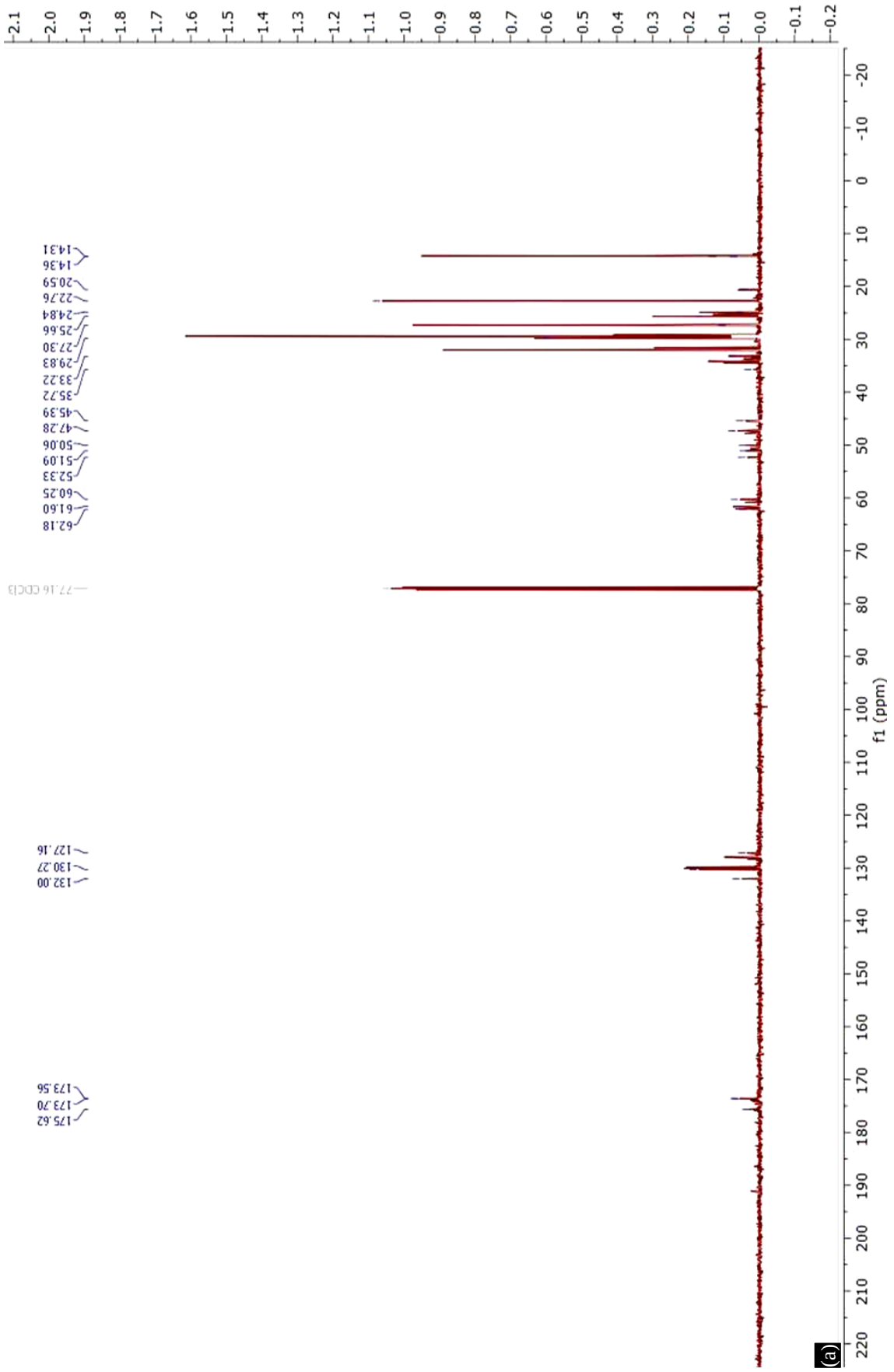

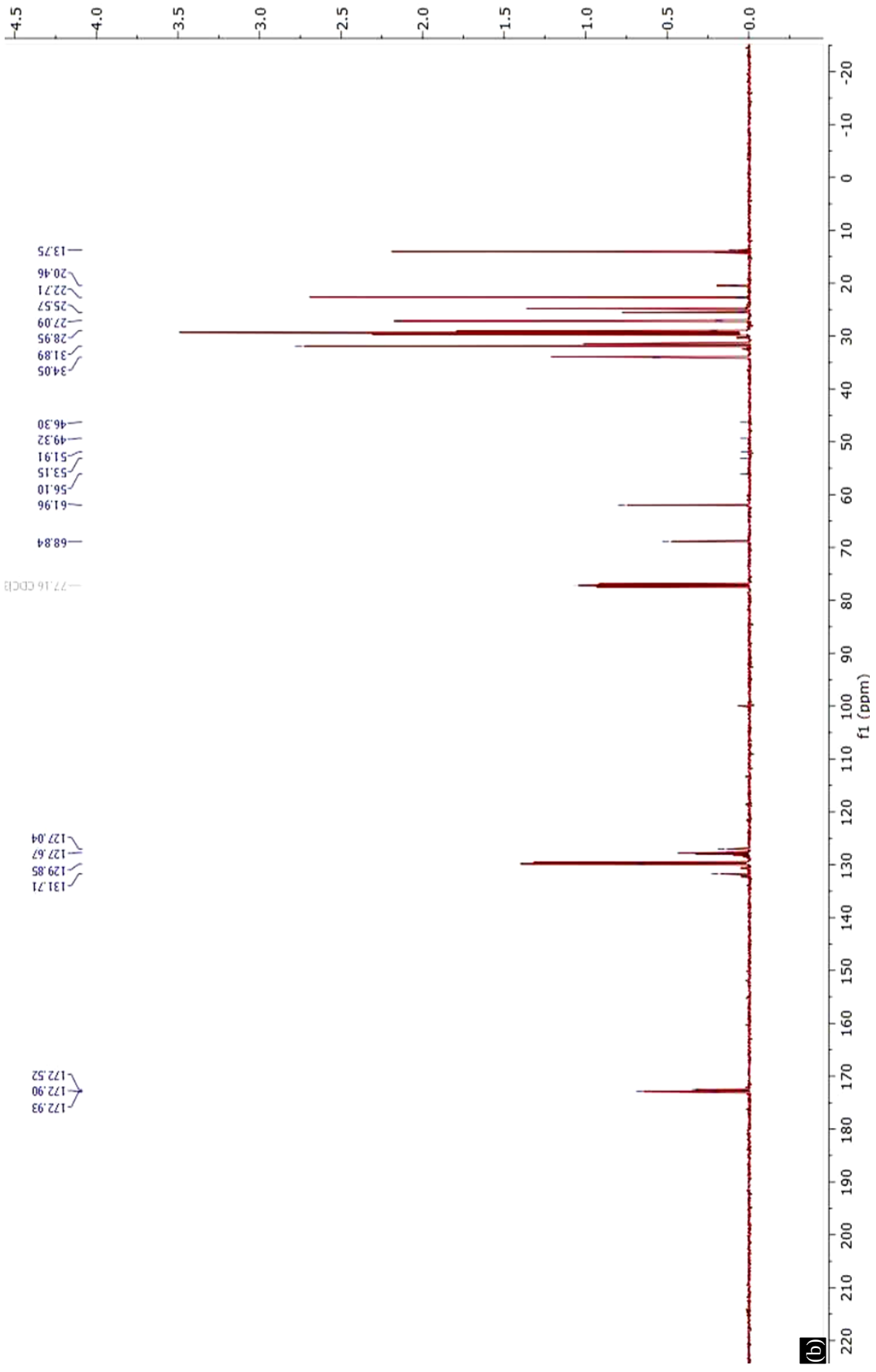

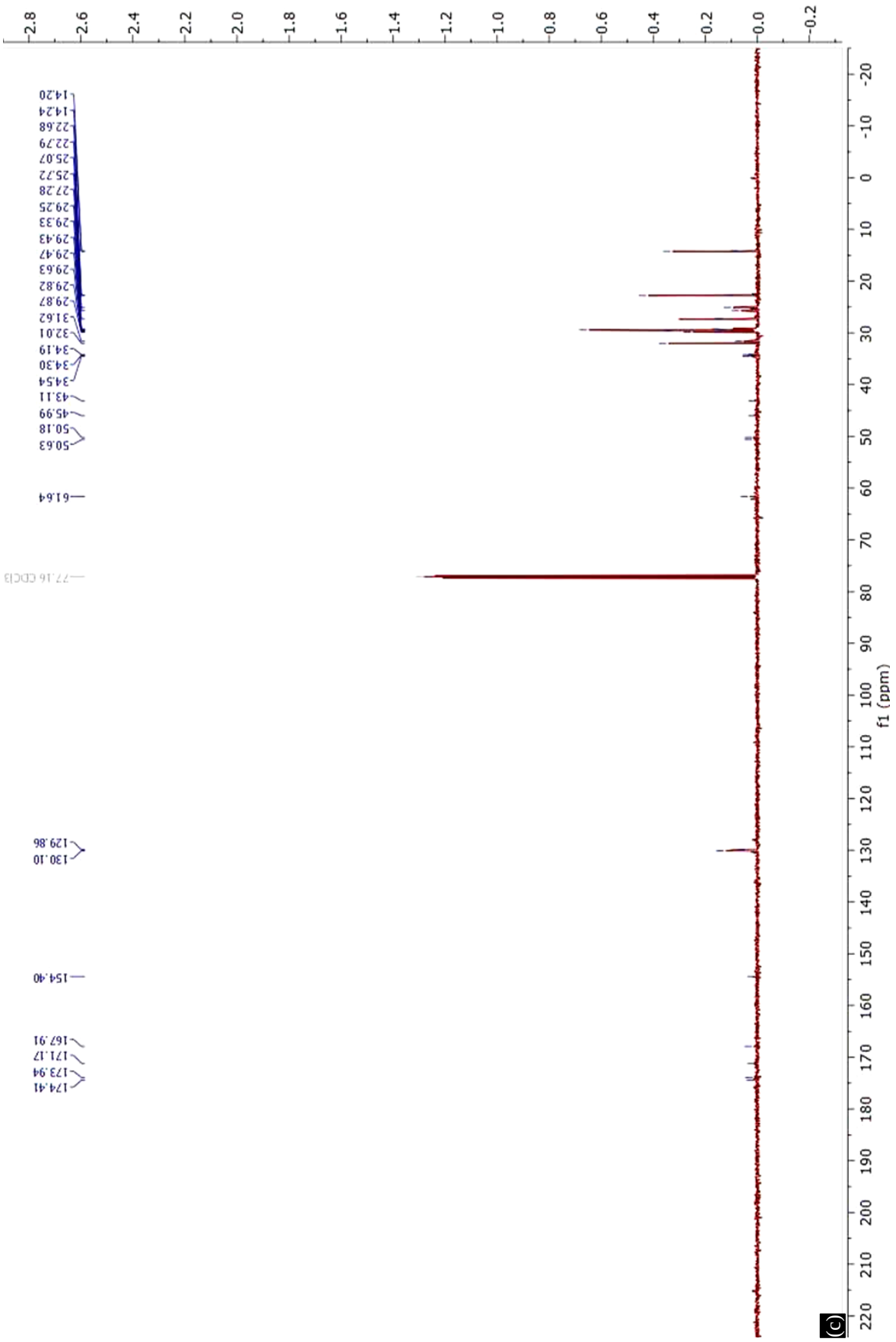

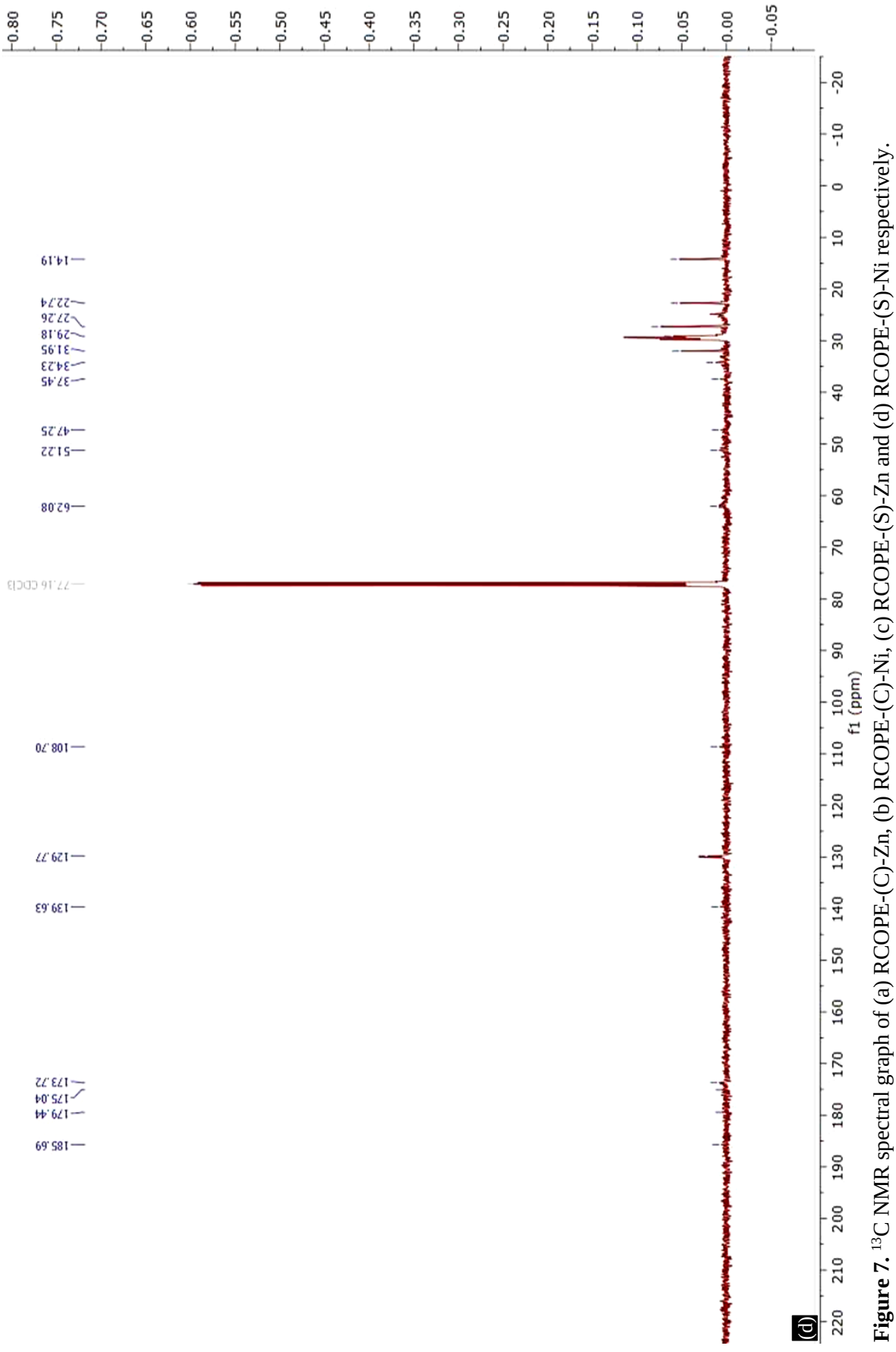

Figure 7. ^{13}C NMR spectral graph of (a) RCOPE-(C)-Zn, (b) RCOPE-(C)-Ni, (c) RCOPE-(S)-Zn and (d) RCOPE-(S)-Ni respectively.

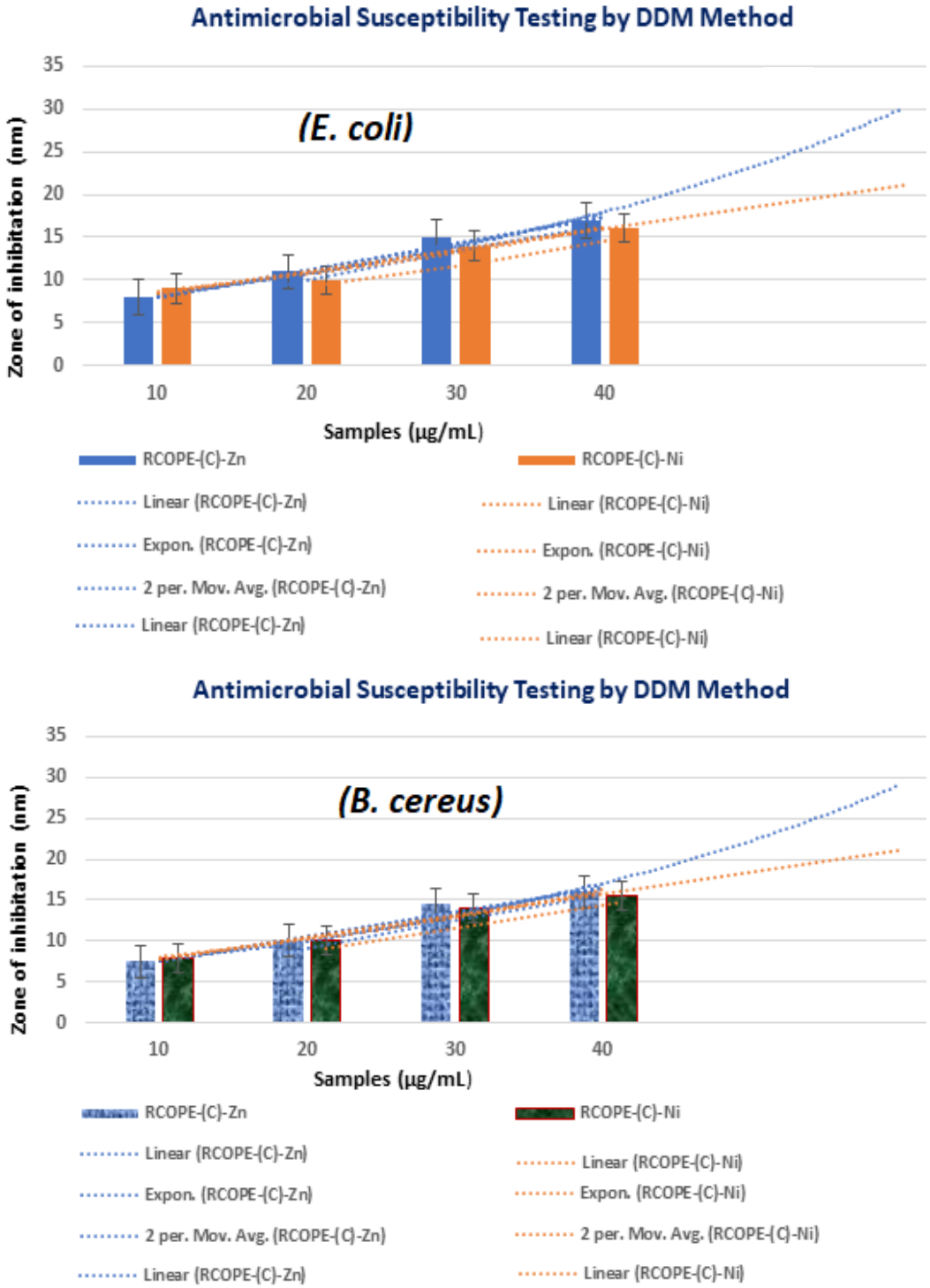

Figure 8. Antibacterial resistances of RCOPE-(C)-Zn & RCOPE-(C)-Ni against *Escherichia coli (E. coli)* (G-ve) and *Bacillus cereus (B. cereus)* (G+ve).

Increased antibacterial activity is due to metal ions being released from the polymer matrix, where they had been loosely bound by the O-M coordination site, so they look for interactions with cells that are more favourable from a thermodynamic point of view. The results showed significant antibacterial activity to be utilised as the antibacterial agents look for interactions with cells that are more favourable from a thermodynamic point of view. Significant bactericidal property was identified, suggesting that these synthetic materials might be used as antibiotics.

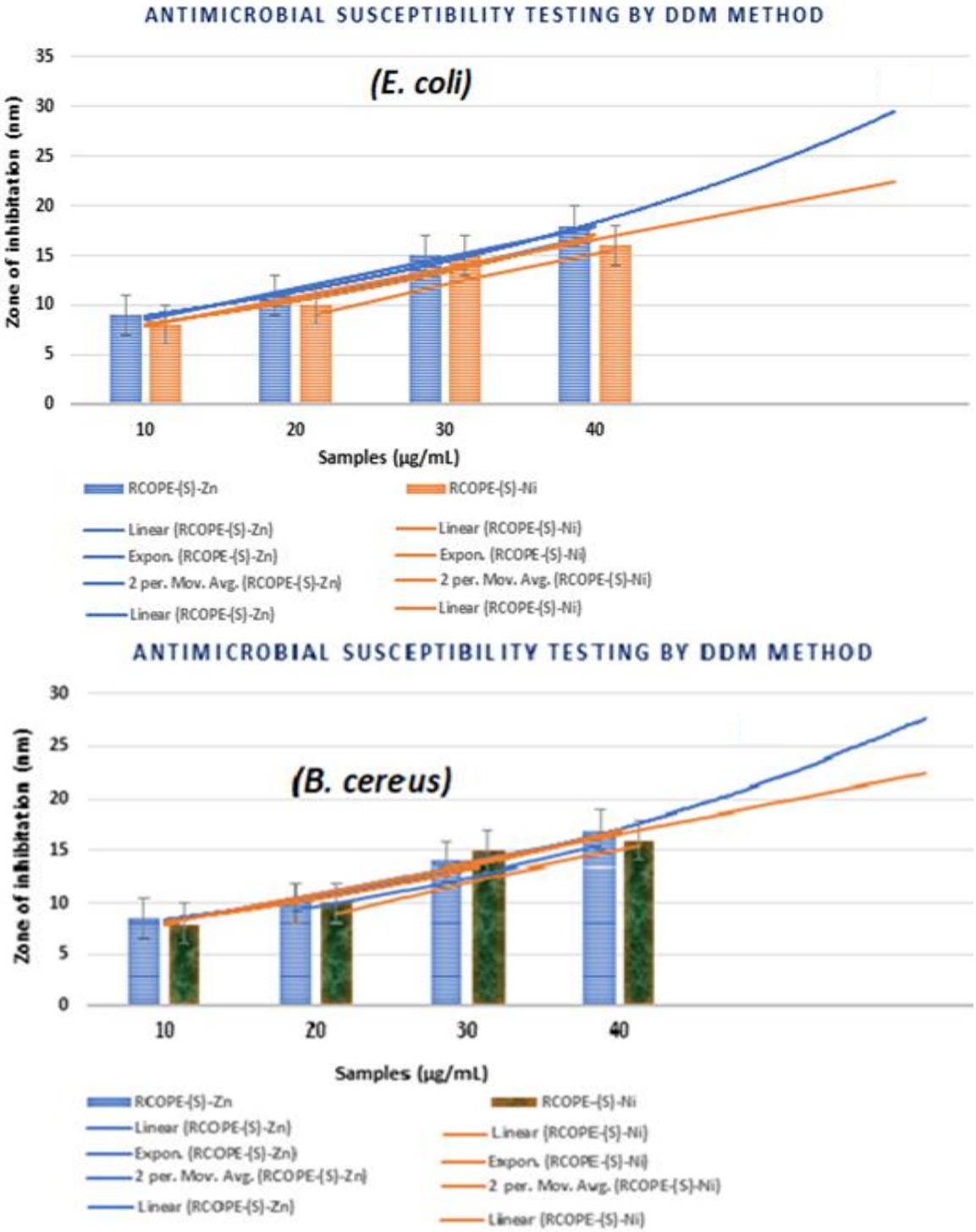

Figure 9. Antibacterial resistances of RCOPE-(S)-Zn & RCOPE-(S)-Ni against *Escherichia coli (E. coli)* (G-ve) and *Bacillus cereus (B. cereus)* (G+ve).

CONCLUSION

Canola oil based polymeric matrix was successfully synthesised with citric acid and succinic acid and henceforth, were incorporated with divalent metal ions- Zinc and Nickel at elevated temperatures. The structures were well established with FTIR, UV-Visible, ^{1}H and ^{13}C NMR spectra and band gap energies were also determined. DLS studies suggest that these metal-incorporated poly-(Citrate/Succinate)-amide could be further studied for therapeutic delivery systems.

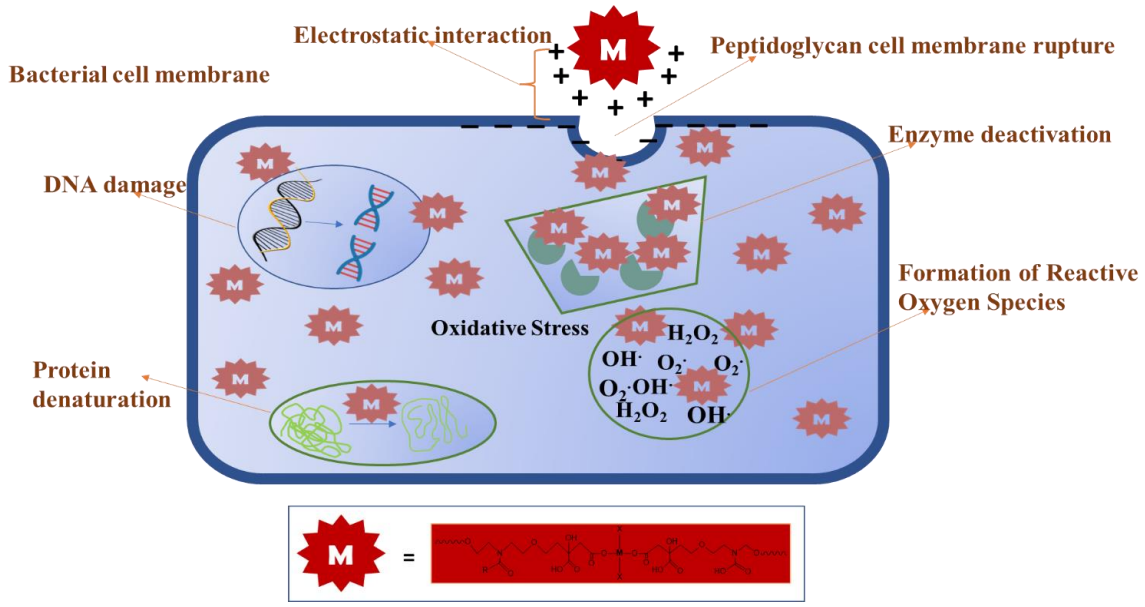

Figure 10. Proposed antibacterial activity mechanism of the synthesised complexes [26, 50].

Although it is an important and difficult task to formulate agents with appropriate zeta potential, additions to the membrane can alter the charge of the phospholipid bilayer. And with suitable alterations, these fabricated samples might be studied for their utility in the field of antibacterial drug-delivery agents. The Zinc and Nickel incorporated complexes of citric acid and succinic acid [RCOPE-(C)-Zn, RCOPE-(C)-Ni, RCOPE-(S)-Zn and RCOPE-(S)-Ni] showed sufficient potency against G+ve bacteria *B. cereus* (MCC2243) and the G-ve bacteria *E. coli* (MCC2412). In both the cases, zinc incorporated complexes [RCOPE-(C)-Zn and RCOPE-(S)-Zn] showed slightly better antibacterial activity than nickel incorporated complexes [RCOPE-(C)-Ni and RCOPE-(S)-Ni]. With the increasing in concentration, all the fabricated samples have shown almost similar activity against the bacteria with the increase in concentration. It has been theorised that their, [RCOPE-(C)-Zn and RCOPE-(S)-Zn], remarkable antibacterial action results from the production of antibacterial ions that interact electrostatically with the microbial cell wall, triggering cell destruction. These findings provide compelling evidence that the synthesised metal ions incorporated polymers may have potential as bio-degradable antibacterial agents irrespective of the acid used in the system with beneficial to both the environment and human health when produced using an easy and environmentally benign method, simultaneously being economical.

DECLARATIONS

Ethical Approval and Consent to Participate

'Not applicable'

Consent of publication

'Not applicable'

Availability of Data and Materials

The dataset generated and/or analysed during the current study are available from the corresponding author, upon reasonable request.

Competing interest

The authors declare that there is no conflict of interest.

Funding

'Not applicable'.

Acknowledgment

We would like to acknowledge Jamia Millia Islamia for NON-NET fellowship and AMRC, Mandi for NMR facility. We would also acknowledge CIF, Jamia Millia Islamia for other characterization of samples.

Author Contribution

Juhi Gupta: Conceptualization, methodology, Formal analysis, Data curation, Visualization, and original draft preparation. Archana Chakravarty: Methodology, Formal analysis, Data curation, and Visualization. Md. Ikbal Ahmed Talukdar: Formal analysis, Data curation, and Visualization. Nitu Singh: Formal analysis, Data curation, and Visualization. Athar A. Hashmi: Conceptualization, methodology, supervisor, Formal analysis, Data curation, Visualization, Validation and Reviewing and Editing.

REFERENCES

1. T.M. Gandini, A. and Lacerda, Polymers from Renewable Resources: Macromolecular Materials for the Twenty-First Century?, Macromol. Eng. (2022). https://doi.org/https://doi.org/10.1002/9783527815562.mme0019.
2. J.A.C. Silva, L.M. Grilo, A. Gandini, T.M. Lacerda, The prospering of macromolecular materials based on plant oils within the blooming field of polymers from renewable resources, Polymers (Basel). 13 (2021). https://doi.org/10.3390/polym13111722.
3. M. Finnveden, P. Hendil-Forssell, M. Claudino, M. Johansson, M. Martinelle, Lipase-catalyzed synthesis of renewable plant oil-based polyamides, Polymers (Basel). 11 (2019) 1–9. https://doi.org/10.3390/polym11111730.
4. W. Al-Otaibi, N.M. Alandis, M. Alam, Leucaena leucocephala oil-based poly malate-amide nanocomposite coating material for anticorrosive applications, E-Polymers. 23 (2023). https://doi.org/10.1515/epoly-2023-0036.
5. M. Alam, A. Ghosal, F. Zafar, M. Ahmed, M. Altaf, Preparation of Co(II)/Cu(II) Metal-Based Metallopolymer Nanocomposites: A Protective Coating for Carbon Steel, J. Polym. Environ. 32 (2024) 588–606. https://doi.org/10.1007/s10924-023-02968-x.
6. S.I. Bhat, S. Ahmad, Castor oil-TiO2 hyperbranched poly (ester amide) nanocomposite: a sustainable, green precursor-based anticorrosive nanocomposite coatings, Prog. Org. Coatings. 123 (2018) 326–336. https://doi.org/10.1016/j.porgcoat.2018.06.010.
7. M.A. Manawwer Alam, Fahmina Zafar, Anujit Ghosal, Formulation of silica-based corn oil transformed polyester acryl amide-phenol formaldehyde corrosion resistant coating material, J. Appl. Polym. Sci. 139 (2021). https://doi.org/https://doi.org/10.1002/app.51651.
8. N. Nagabhooshanam, S. Baskar, T.R. Prabhu, S. Arumugam, Evaluation of tribological characteristics of nano zirconia dispersed biodegradable canola oil methyl ester metalworking fluid, Tribol. Int. 151 (2020) 106510. https://doi.org/10.1016/j.triboint.2020.106510.
9. M. Alam, N.M. Alandis, N. Ahmad, F. Zafar, A. Khan, M.A. Alam, Development of hydrophobic, anticorrosive, nanocomposite polymeric coatings from canola oil: A sustainable resource, Polymers (Basel). 12 (2020) 1–15. https://doi.org/10.3390/polym12122886.
10. X. Kong, G. Liu, J.M. Curtis, Novel polyurethane produced from canola oil based poly(ether ester) polyols: Synthesis, characterization and properties, Eur. Polym. J. 48 (2012) 2097–2106. https://doi.org/10.1016/j.eurpolymj.2012.08.012.
11. M.B. Karimi, G. Khanbabaei, G.M.M. Sadeghi, Unsaturated canola oil-based polyol as effective nucleating agent for polyurethane hard segments, J. Polym. Res. 26 (2019). https://doi.org/10.1007/s10965-019-1924-0.
12. T.S. Omonov, J.M. Curtis, Biobased epoxy resin from canola oil, J. Appl. Polym. Sci. 131 (2014) 1–9. https://doi.org/10.1002/app.40142.
13. M.R. López-Cuellar, J. Alba-Flores, J.N.G. Rodríguez, F. Pérez-Guevara, Production of polyhydroxyalkanoates (PHAs) with canola oil as carbon source, Int. J. Biol. Macromol. 48 (2011) 74–80. https://doi.org/10.1016/j.ijbiomac.2010.09.016.

14. R. V. Nimbalkar, V.D. Athawale, Synthesis and characterization of canola oil alkyd resins based on novel acrylic monomer (ATBS), JAOCS, J. Am. Oil Chem. Soc. 87 (2010) 947–954. https://doi.org/10.1007/s11746-010-1573-2.
15. N.A. Lundquist, M.J.H. Worthington, N. Adamson, C.T. Gibson, M.R. Johnston, A. V. Ellis, J.M. Chalker, Polysulfides made from re-purposed waste are sustainable materials for removing iron from water, RSC Adv. 8 (2018) 1232–1236. https://doi.org/10.1039/c7ra11999b.
16. S. Ghobadi, Z. Hassanzadeh-Rostami, F. Mohammadian, M. Zare, S. Faghih, Effects of Canola Oil Consumption on Lipid Profile: A Systematic Review and Meta-Analysis of Randomized Controlled Clinical Trials, J. Am. Coll. Nutr. 38 (2019) 185–196. https://doi.org/10.1080/07315724.2018.1475270.
17. N. Ahmad, M. Saleem, B.M. Atta, S. Mahmood, Characterization of Desi Ghee Extracted by Different Methods Using Fluorescence Spectroscopy, J. Fluoresc. 29 (2019) 1411–1421. https://doi.org/10.1007/s10895-019-02453-6.
18. M.N.A. Eskin, F. Aladedunye, E.H. Unger, S. Shah, G. Chen, P.J. Jones, Canola Oil, Bailey's Ind. Oil Fat Prod. (2020) 1–63. https://doi.org/10.1002/047167849x.bio004.pub2.
19. J. Dupont, P.J. White, K.M. Johnston, D.H. Alexander Heggtveit, B.E. McDonald, S.M. Grundy, A. Bonanome, Food Safety and Health Effects of Canola Oil, J. Am. Coll. Nutr. 8 (1989) 360–375. https://doi.org/10.1080/07315724.1989.10720311.
20. D. Yu, J. Chen, Q. Zhou, X. Wang, Y. Chen, L. Wang, B. Yu, Catalytic transfer hydrogenation of low-erucic-acid rapeseed oil over a ni-ag0.15/sba15 catalyst, J. Oleo Sci. 69 (2020) 1191–1198. https://doi.org/10.5650/jos.ess20055.
21. J.J.S. Nurhan Turgut Dunford, Enrique Martínez-Force, High-oleic sunflower seed oil, in: Frank J. Flider (Ed.), High Oleic Oils, AOCS Press, 2022: pp. 109–124. https://doi.org/https://doi.org/10.1016/B978-0-12-822912-5.00004-6.
22. N.P. Bharathi, M. Alam, S. Shreaz, A.A. Hashmi, Synthesis, characterization and biological studies of oil based Tin polymer, J. Inorg. Organomet. Polym. Mater. 19 (2009) 459–465. https://doi.org/10.1007/s10904-009-9288-2.
23. M.A. Malik, O.A. Dar, P. Gull, M.Y. Wani, A.A. Hashmi, Heterocyclic Schiff base transition metal complexes in antimicrobial and anticancer chemotherapy, Medchemcomm. 9 (2018) 409–436. https://doi.org/10.1039/c7md00526a.
24. T. Singh, S. Shreaz, A.A. Hashmi, Synthesis of sunflower oil based bimetallic polymer and its antifungal studies, Int. J. Polym. Mater. Polym. Biomater. 62 (2013) 653–662. https://doi.org/10.1080/00914037.2013.769168.
25. M. Faisal, Shah; Sadiq, Saima; Mustafa, Muhammad; Khan, M.H.; Sadiq, Muhammad; Iqbal, Zaffar; Khan, Tailoring the antibacterial and antioxidant activities of iron nanoparticles with amino benzoic acid, RSC Sustain. (2022).
26. M.I.A. Talukdar, I. Ahamad, S. Iqbal, M.A. Malik, O.A. Dar, M. Khursheed Akram, T. Fatma, A.A. Hashmi, Fabrication of metal incorporated polymer composite: An excellent antibacterial agent, J. Mol. Struct. 1225 (2021). https://doi.org/10.1016/j.molstruc.2020.129091.
27. Y. Mageshwaran, V., Sivasubramanian, P., Kumar, P., Nagaraju, Antibacterial Response of Nanostructured Chitosan Hybrid Materials., in: A. Swain, S.K., Biswal (Ed.), Chitosan Nanocomposites. Biol. Med. Physics, Biomed. Eng., Springer, Singapore, 2023: pp. 161–179. https://doi.org/https://doi.org/10.1007/978-981-19-9646-7_7.
28. N. Sharmin, J.T. Rosnes, L. Prabhu, U. Böcker, M. Sivertsvik, Effect of Citric Acid Cross Linking on the Mechanical, Rheological and Barrier Properties of Chitosan, Molecules. 27 (2022) 1–16. https://doi.org/10.3390/molecules27165118.
29. L. Wen, Y. Liang, Z. Lin, D. Xie, Z. Zheng, C. Xu, B. Lin, Design of multifunctional food packaging films based on carboxymethyl chitosan/polyvinyl alcohol crosslinked network by using citric acid as crosslinker, Polymer (Guildf). 230 (2021) 124048. https://doi.org/10.1016/j.polymer.2021.124048.
30. M.C. Anandarup Goswami, Chandrasekar Kuppan, Shajeeya Amren Shaik, Greener synthesis at different scales, in: O.K. Boris Kharisov (Ed.), Handb. Greener Synth. Nanomater. Compd., Elsevier, 2021: pp. 63–106. https://doi.org/https://doi.org/10.1016/B978-0-12-821938-6.00003-7.

31. M. Latos-Brozio, A. Masek, Environmentally friendly polymer compositions with natural amber acid, Int. J. Mol. Sci. 22 (2021) 1–17. https://doi.org/10.3390/ijms22041556.
32. M.A. Sawpan, Polyurethanes from vegetable oils and applications: a review, J. Polym. Res. 25 (2018). https://doi.org/10.1007/s10965-018-1578-3.
33. S. Zafar, F., Ashraf, S. M., & Ahmad, Studies on zinc-containing linseed oil based polyesteramide., React. Funct. Polym. 67 (2007) 928–935. https://doi.org/10.1016/j.reactfunctpolym.2007.05.018.
34. I.H. Ifijen, H.D. Odi, M. Maliki, S.O. Omorogbe, A.I. Aigbodion, E.U. Ikhuoria, Correlative studies on the properties of rubber seed and soybean oil-based alkyd resins and their blends, J. Coatings Technol. Res. 18 (2021) 459–467. https://doi.org/10.1007/s11998-020-00416-2.
35. B. Ozcelik, E. Kuram, E. Demirbas, E. Şik, Effects of vegetable-based cutting fluids on the wear in drilling, Sadhana - Acad. Proc. Eng. Sci. 38 (2013) 687–706. https://doi.org/10.1007/s12046-013-0179-4.
36. O.H. Al-obaidi, Synthesis , Characterization , Theoretical And Antimicrobial Evaluation Of New Co (Ii), Ni (Ii) And Cu (Ii) Complexes Of Flavylium Salt, Int. Res. J. Apllied Basic Sci. 8 (2014) 88–92. https://doi.org/10.11648/j.ijbbmb.20160101.15.
37. L. Kletsch, R. Jordan, A.S. Köcher, S. Buss, C.A. Strassert, A. Klein, Photoluminescence of ni(Ii), pd(ii), and pt(ii) complexes [m(me2dpb)cl] obtained from c-h activation of 1,5-di(2-pyridyl)-2,4-dimethylbenzene (me2dpbh), Molecules. 26 (2021). https://doi.org/10.3390/molecules26165051.
38. M.D. Allendorf, M.E. Foster, F. Léonard, V. Stavila, P.L. Feng, F.P. Doty, K. Leong, E.Y. Ma, S.R. Johnston, A.A. Talin, Guest-induced emergent properties in metal-organic frameworks, J. Phys. Chem. Lett. 6 (2015) 1182–1195. https://doi.org/10.1021/jz5026883.
39. R.E. Malekshah, F. Shakeri, A. Khaleghian, M. Salehi, Developing a biopolymeric chitosan supported Schiff-base and Cu(II), Ni(II) and Zn(II) complexes and biological evaluation as pro-drug, Int. J. Biol. Macromol. 152 (2020) 846–861. https://doi.org/10.1016/j.ijbiomac.2020.02.245.
40. R. Raj kumar, Ramasamy; Kasim, Mohamed; Subarkhan, Mohamed; Ramesh, Synthesis and Structure of Nickel(II) thiocarboxamide Complexes: Effect of ligand substitutions on DNA/Protein binding, Antioxidant and Cytotoxicity, RSC Adv. (2012). https://doi.org/10.1039/x0xx00000x.
41. A.H. Ahmed, A.M. Hassan, H.A. Gumaa, B.H. Mohamed, A.M. Eraky, Nickel(II)-oxaloyldihydrazone complexes: Characterization, indirect band gap energy and antimicrobial evaluation, Cogent Chem. 2 (2016) 1142820. https://doi.org/10.1080/23312009.2016.1142820.
42. M. Armstrong, S. Mahadevan, N. Selvapalam, C. Santulli, S. Palanisamy, C. Fragassa, Augmenting the double pipe heat exchanger efficiency using varied molar Ag ornamented graphene oxide (GO) nanoparticles aqueous hybrid nanofluids, Front. Mater. 10 (2023). https://doi.org/10.3389/fmats.2023.1240606.
43. I.M. Mahbubul, Stability and Dispersion Characterization of Nanofluid, William Andrew Publishing, 2019. https://doi.org/10.1016/b978-0-12-813245-6.00003-4.
44. A. Barhoum, M.L. García-Betancourt, H. Rahier, G. Van Assche, Physicochemical characterization of nanomaterials: Polymorph, composition, wettability, and thermal stability, in: A.S.H.M. Ahmed Barhoum (Ed.), Emerg. Appl. Nanoparticles Archit. Nanostructures Curr. Prospect. Futur. Trends, Elsevier, 2018: pp. 255–278. https://doi.org/10.1016/B978-0-323-51254-1.00009-9.
45. K. Pate, P. Safier, Chemical metrology methods for CMP quality, in: Suryadevara Babu (Ed.), Adv. Chem. Mech. Planarization, SECOND, Woodhead Publishing Series, 2021: pp. 355–383. https://doi.org/10.1016/B978-0-12-821791-7.00017-4.
46. E.M.A. Dannoun, S.B. Aziz, M.A. Brza, M.M. Nofal, A.S.F.M. Asnawi, Y.M. Yusof, S. Al-Zangana, M.H. Hamsan, M.F.Z. Kadir, H.J. Woo, The study of plasticized solid polymer blend electrolytes based on natural polymers and their application for energy storage EDLC devices, Polymers (Basel). 12 (2020) 1–19. https://doi.org/10.3390/polym12112531.
47. M.M. Tosi, A.P. Ramos, B.S. Esposto, S.M. Jafari, Dynamic light scattering (DLS) of nanoencapsulated food ingredients, Elsevier Inc., 2020. https://doi.org/10.1016/b978-0-12-815667-4.00006-7.
48. Haseena, A. Khan, F. Aslam, T. Kanwal, M.R. Shah, A.A. Khan Khalil, S.W. Ali Shah, E.M. Alshammari, E.A. El-Masry, G.E.S. Batiha, R.S. Baty, Enhanced antibacterial potential of

amoxicillin against helicobacter pylori mediated by lactobionic acid coated zn-mofs, Antibiotics. 10 (2021) 1–13. https://doi.org/10.3390/antibiotics10091071.
49. M. Alam, N. M Alandis, E. Sharmin, N. Ahmad, F.M. Husain, A. Khan, Mechanically Strong, Hydrophobic, Antimicrobial, and Corrosion Protective Polyesteramide Nanocomposite Coatings from Leucaena leucocephala Oil: A Sustainable Resource, ACS Omega. 5 (2020) 30383–30394. https://doi.org/10.1021/acsomega.0c03333.
50. S.M. Dizaj, F. Lotfipour, M. Barzegar-Jalali, M.H. Zarrintan, K. Adibkia, Antimicrobial activity of the metals and metal oxide nanoparticles, Mater. Sci. Eng. C. 44 (2014) 278–284. https://doi.org/10.1016/j.msec.2014.08.031.

